

https://dspace.org/

Burning Cleaning Dumping and Dissolution Site Formation Processes and Stratigraphy of pre110000YearOldMSA 1 Deposits in Cave 1 Klasies River Main Site in South Africa

Peter Morrissey; Sarah Wurz; B Ligouis; S Mentzer

https://hdl.handle.net/10539/47613
WOS

Downloaded from a DSpace repository. https://dspace.org/

Check for updates

Geoarchaeology

WILEY

Geoarchaeology An International Journal

RESEARCH ARTICLE OPEN ACCESS

Burning, Cleaning, Dumping, and Dissolution: Site Formation Processes and Stratigraphy of Pre-110,000-Year-Old MSA 1 Deposits in Cave 1, Klasies River Main Site, South Africa

Peter Morrissey[1] | Sarah Wurz[1,2] | Bertrand Ligouis[3,4] | Susan M. Mentzer[3]

[1]School of Geography, Archaeology and Environmental Studies, University of the Witwatersrand, Johannesburg, South Africa | [2]SFF Centre for Early Sapiens Behaviour (SapienCE), University of Bergen, Bergen, Norway | [3]Senckenberg Centre for Human Evolution and Palaeoenvironment, Institute for Archaeological Sciences, Department of Geosciences, Eberhard Karls Universität Tübingen, Tübingen, Germany | [4]Laboratory for Applied Organic Petrology (LAOP), Tübingen, Germany

Correspondence: Peter Morrissey (peter.morrissey@wits.ac.za)

Received: 18 December 2023 | **Revised:** 14 February 2025 | **Accepted:** 22 February 2025

Scientific Editor: Dr. Justin Holcomb

Funding: This work was supported by GENUS: DSI-NRF Centre of Excellence in Palaeosciences, Grant Number: UID 86073; Ministerium für Wissenschaft, Forschung und Kunst Baden-Württemberg; and the Palaeontological Scientific Trust (PAST).

Keywords: archaeological micromorphology | combustion features | diagenesis | Klasies River | Middle Stone Age | site formation processes

ABSTRACT

Understanding the formation and stratigraphy of sequences in southern African Middle Stone Age (MSA) sites is vital for contextualizing evidence for the evolution of modern human behaviors and cognition. Deposits at these sites often have complex formation histories, typically involving a range of anthropogenic, geogenic, and biogenic depositional and post-depositional processes, and micro-laminated deposits are common. Consequently, archaeological micromorphology and related micro-analyses are now routinely a major component of MSA geoarchaeological research in the region. In the past few decades, microscale studies of the formation of anthropogenic features and deposits at MSA sites have begun to provide important behavioral information, including evidence for varying occupational intensities and the structuring and maintenance of living spaces. Here, a microscale geoarchaeological approach is applied to deposits dating to the MSA I cultural phase (> 110 ka) in the Cave 1 Witness Baulk. The results show that humans played a considerable role in site formation and that subsequent diagenesis affected the guano, charcoal, ash, and shell, with particular impact on the carbonates which were variably dissolved, altered, or recrystallized. This latter process helped to preserve ash through reduced dissolution potential. Spatial and temporal patterns in these factors influence the macroscopic properties of the deposits in any particular area, with significant implications for the correlation of extant deposits across areas excavated at low resolution during the 1960s. Different, variably preserved, anthropogenic features and deposits were found to make up a significant proportion of the deposits. Inferred behaviors range from repeated long-term low-intensity use of individually stacked hearths to the formation of dumped deposits (including shell middens) due to repeated hearth maintenance and patterned discarding of food waste during more intensive occupations. Differences in occupational intensity and frequency both within and between the two recognized MSA I members could indicate adaptation to changing conditions as temperatures and sea levels fluctuated during Marine Isotope Stage 5e and early Stage 5d, but changes in geogenic depositional rates over the same period could skew our perception of occupational frequency. The current limited and low-resolution

This is an open access article under the terms of the Creative Commons Attribution-NonCommercial-NoDerivs License, which permits use and distribution in any medium, provided the original work is properly cited, the use is non-commercial and no modifications or adaptations are made.

© 2025 The Author(s). *Geoarchaeology* published by Wiley Periodicals LLC.

dating evidence prevents correlation with any specific event/s, which might have affected behavior and/or depositional rates.

1 | Introduction

Klasies River Main site (KRM), on South Africa's southern Cape coast (Figure 1), is well known for its Late Pleistocene deposits, which have yielded important *Homo sapiens* fossils, large informative Middle Stone Age (MSA) archaeological assemblages, and significant palaeoenvironmental data sets (Singer and Wymer 1982; Deacon and Geleijnse 1988; Deacon 1989; Grine et al. 2017; Wurz 2023). Evidence from KRM has played an important role in the characterization and contextualization of MSA human behavior during a significant period for understanding cognitive evolution (Deacon 1995; McBrearty and Brooks 2000; Wadley 2015; Scerri and Will 2023). The site complex, comprising five closely associated caves and rockshelters, has seen extensive fieldwork in three phases: 1967–1968 (Singer and Wymer 1982), 1984–1995 (Deacon 1995), and 2013–present (Wurz et al. 2018, 2022). The scale of excavation, recording, and interpretation has varied, with implications for understanding stratigraphy across the site complex (Morrissey et al. 2022).

All three phases of investigation have included geoarchaeological research. Both the initial study and Deacon's work were based on macroscopic field descriptions and bulk sample analysis, with the former particularly focused on reconstructing environmental conditions (Butzer 1982) and the latter placing greater emphasis on the impacts of site formation processes on human fossils and archaeological assemblages (Deacon and Geleijnse 1988; Deacon 2008). The second phase also resulted in behavioral interpretations of

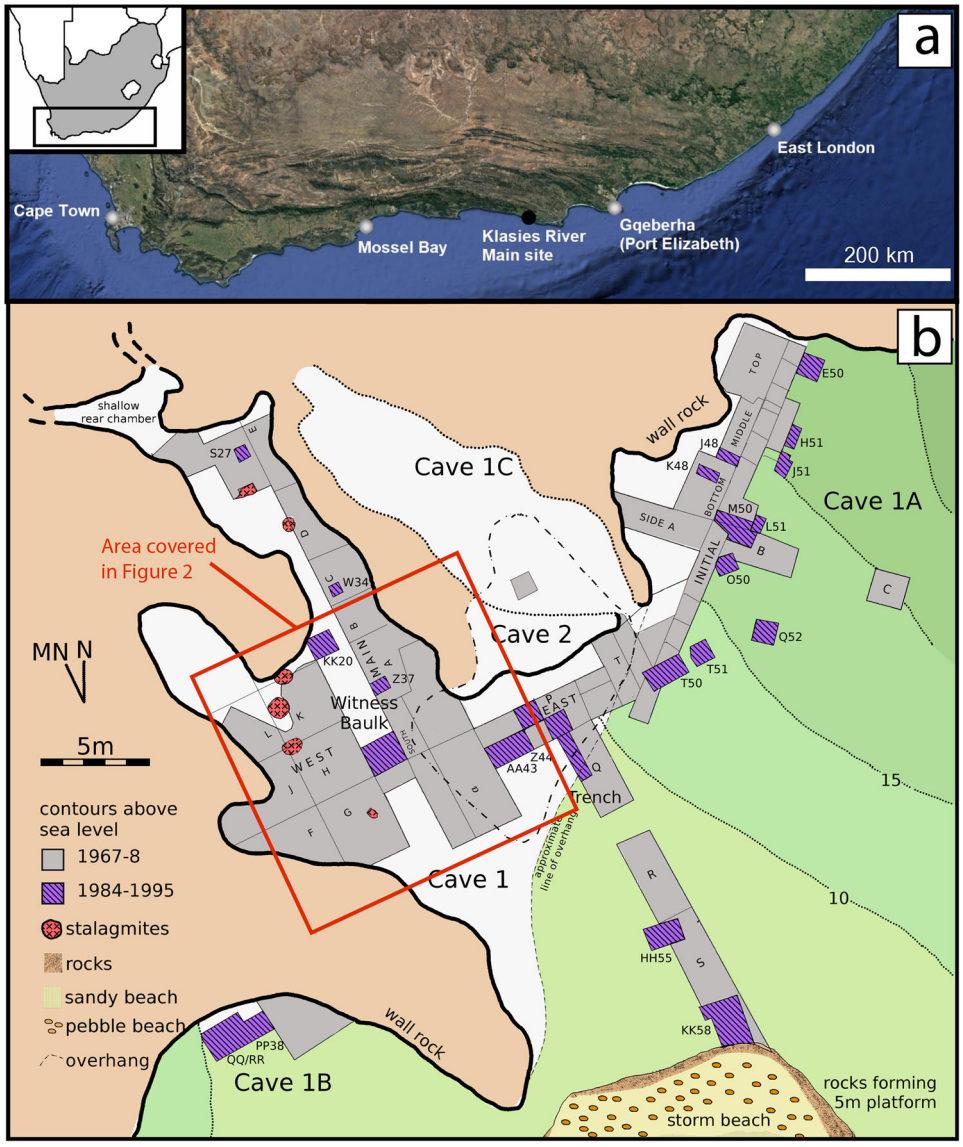


FIGURE 1 | (a) Location of the Klasies River Main site along South Africa's southern Cape coast. (b) Map of the Klasies River Main site complex (after Wurz et al. 2018). See Figure 2 for a more detailed view of Cave 1, including the locations of samples used in this study.

15206548, 2025, 2, Downloaded from https://onlinelibrary.wiley.com/doi/10.1002/gea.70005 by University Of Witwatersrand, Wiley Online Library on [22/10/2025]. See the Terms and Conditions (https://onlinelibrary.wiley.com/terms-and-conditions) on Wiley Online Library for rules of use; OA articles are governed by the applicable Creative Commons License

some anthropogenic features (Henderson 1992; Deacon 1993, 1995). The on-going Wurz research program coincided with a rapid increase in the application of archaeological micromorphology and related micro-analyses at MSA sites in southern Africa (e.g., Miller et al. 2013, 2016; Karkanas et al. 2015, 2021; Haaland et al. 2017, 2021), which followed the success of the first applications of microscale geoarchaeological techniques in the region at Die Kelders (Goldberg 2000), Sibhudu Cave (Goldberg et al. 2009), and Pinnacle Point 13B (Karkanas and Goldberg 2010). Micromorphology, integrated organic petrology, micro-x-ray-fluorescence (μXRF), and micro-Fourier transform infrared spectroscopy (μFTIR) analysis have been applied to different areas of the KRM complex (Larbey et al. 2019; Wurz et al. 2022; Morrissey et al. 2023). The results provide detailed information on the formation histories of the sampled deposits, including insight into diagenesis and evidence for a range of human behaviors.

This study focuses on deposits associated with the MSA I (Figures 2 and 3), the oldest cultural phase (Singer and Wymer 1982; Wurz 2002). They are currently exposed in Caves 1, 1/1 A, and 1B and contain lithic technology characterized by the production of elongated, relatively thin curved blades and points. The technology was geared toward thinning platforms at the dorsal surface through step flaking and rubbing, resulting in significantly different platform-to-length ratios of points and blades in this industry compared to the overlying MSA II or Mossel Bay technocomplex (Wurz et al. 2003). Associated human remains include skull fragments from Cave 1, two maxillary fragments from Cave 1/1 A, and the mandible KRM 41815 from Cave 1B (Grine et al. 2017). Anthropogenic features are poorly preserved in Cave 1B (Morrissey et al. 2023), but preservation is far better in Cave 1 (Deacon and Geleijnse 1988; Larbey et al. 2019; Wurz et al. 2022).

Published microscale observations for Cave 1 (Larbey et al. 2019; Wurz et al. 2022) come from samples collected from the southern end of the Witness Baulk and the Cave 1/1 A boundary (Figure 2). These studies focused on human behaviors involved in forming a few anthropogenic features and subsequent impacts of post-depositional processes. The very limited microscale information on geogenic deposits in Cave 1 means that there is a significant bias toward using macroscale data to interpret their formation histories. However, these descriptions and interpretations are very broad (Singer and Wymer 1982; Butzer 1982; Deacon and Geleijnse 1988) and do not address spatial variation in sedimentary properties observed in the field.

Here, we reconstruct the formation of MSA I deposits deeper into Cave 1, exposed on the western and eastern faces of the Witness

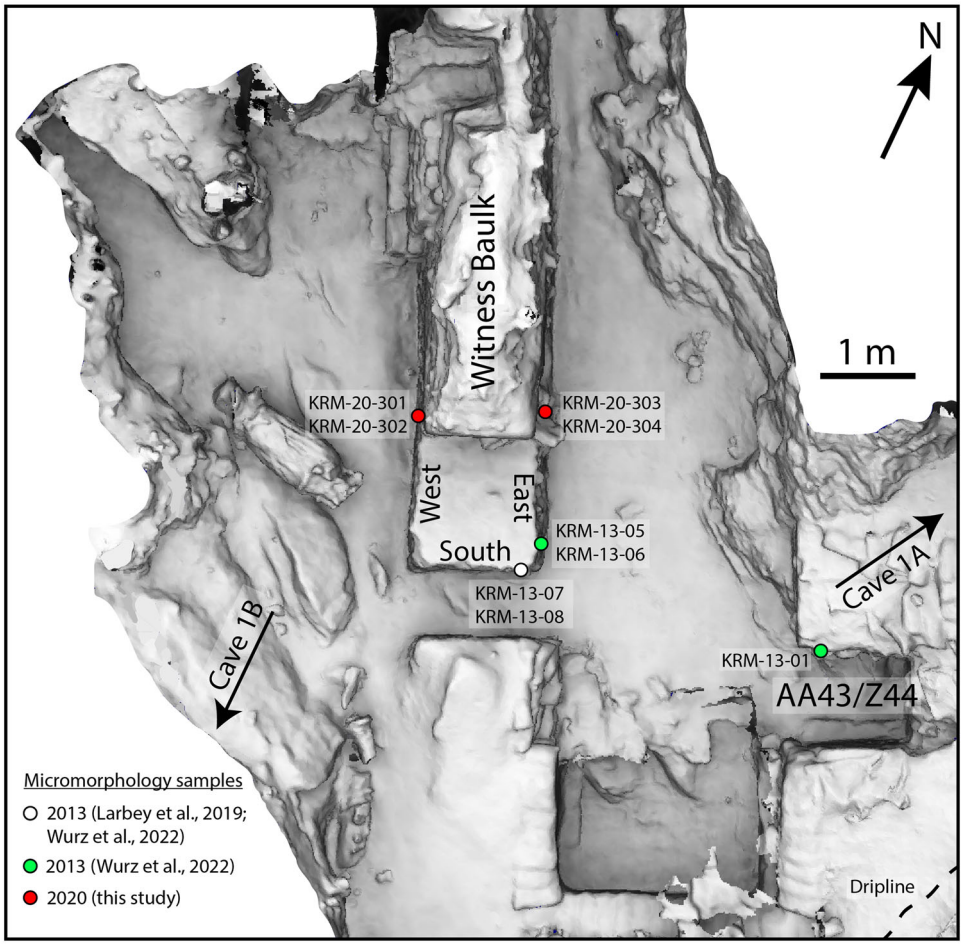


FIGURE 2 | Cave 1 at the Klasies River Main site with the locations of micromorphology samples collected from the MSA I deposits in the Witness Baulk and the AA43/Z44 excavation at the Cave 1/1 A boundary (Imagery from 3D scanning by the Zamani Project). Unlike Cave 1 A, Cave 1B is separated from Cave 1 by the host rock. Note that only KRM-13-07 was analyzed by Larbey et al. (2019). Most of the cave was excavated to bedrock (Singer and Wymer 1982), with subsequent higher-resolution excavations in AA43/Z44 and (ongoing) the Witness Baulk (Wurz et al. 2018).

15206548, 2025, 2, Downloaded from https://onlinelibrary.wiley.com/doi/10.1002/gea.70005 by University Of Witwatersrand, Wiley Online Library on [22/10/2025]. See the Terms and Conditions (https://onlinelibrary.wiley.com/terms-and-conditions) on Wiley Online Library for rules of use; OA articles are governed by the applicable Creative Commons License

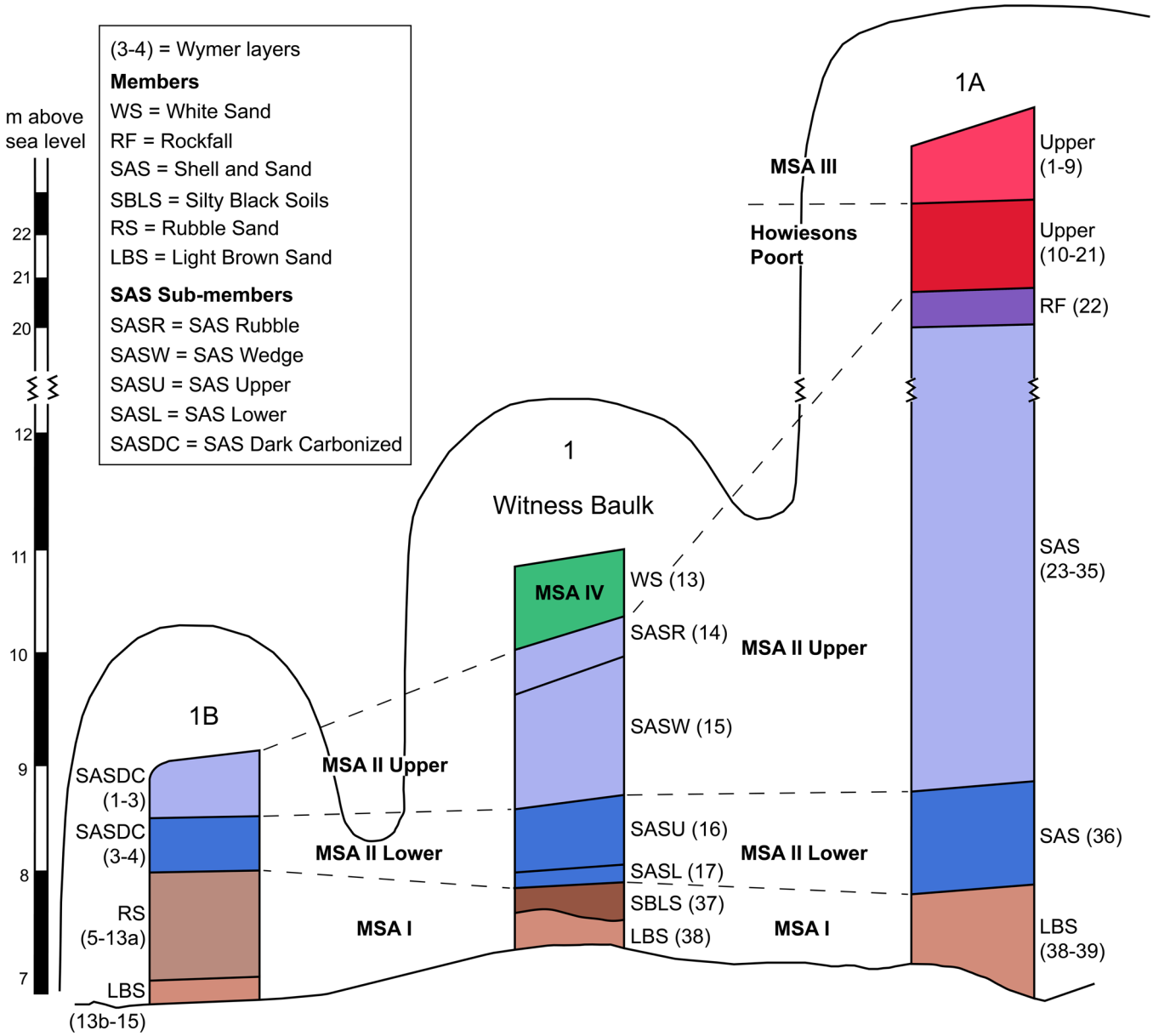


FIGURE 3 | Generalized lithostratigraphy and cultural stratigraphy of Caves 1, 1 A, and 1B at the Klasies River Main site (after Morrissey et al. 2023). Cave 2 is not shown but is above Cave 1 and contains deposits assigned to the Rockfall and Upper Members.

Baulk (Figure 2). Our goals are to provide greater insight into geogenic deposition in the center of Cave 1, to broaden the understanding of anthropogenic site formation processes during the MSA I, and to determine the nature, extent, and impacts of diagenesis on the studied deposits.

2 | Site Context

Cave 1 extends roughly 25 m into the hosting quartzite cliff. It is ~10 m wide at its mouth and ~6 m above the mean sea level at its lowest point. There is no distinct boundary with Cave 1A, an overhang immediately to the east, but Cave 1B, to the southwest, is physically separated by the host rock.

The quartzite cliff is overlain by aeolianites, which have undergone varying degrees of weathering and pedogenesis and are the primary source of secondary calcite (Butzer 1982; Deacon and Geleijnse 1988). Calcium-enriched groundwater reaches Cave 1 via joints and cracks in the otherwise impervious quartzite. Water forms speleothems inside the cave and within the joints and cracks. This creates the potential for the movement of drip locations if routes fill with precipitated calcite or are re-opened by relatively acidic groundwater (Butzer 1982).

In Cave 1, the MSA I is associated with two published lithostratigraphic members. The Light Brown Sand (LBS) Member (Layer 38) lies on either bedrock or basal gravel and is characterized by light yellowish-brown sands with distinct ash and/or shell layers (Singer and Wymer 1982; Deacon and Geleijnse 1988). It is overlain (sometimes unconformably) by darker sediments, which were excavated as Layer 37 by Singer and Wymer (1982) and placed into the Rubble Brown Sand (RBS) Member by Deacon and Geleijnse (1988). The

15206548, 2025, 2, Downloaded from https://onlinelibrary.wiley.com/doi/10.1002/gea.70005 by University Of Witwatersrand, Wiley Online Library on [22/10/2025]. See the Terms and Conditions (https://onlinelibrary.wiley.com/terms-and-conditions) on Wiley Online Library for rules of use; OA articles are governed by the applicable Creative Commons License

RBS is more diverse and complex than its basic and very localized description suggests (Morrissey et al. 2022) and is currently being re-evaluated. The excavated portion of these deposits is now named the Silty Black Soils[1] (SBLS) (Wurz et al. 2022).

The MSA I has been associated with MIS 5e and 5d (130–105 ka) based on both absolute and relative dating (see reviews in Grine et al. 2017; Morrissey et al. 2022). However, a range of contextual and/or methodological concerns have been raised over some dates (Thackeray 1992; Morrissey et al. 2023). Recent well-contextualized uranium–thorium dates indicate that all the MSA I deposits in Cave 1 (and the lowermost of the overlying MSA II deposits) pre-date 110 ka (Wurz et al. 2022). It has generally been assumed that the deposits at KRM must post-date the Last Interglacial highstand at ~120 ka because any older deposits would have been eroded due to higher sea levels (Singer and Wymer 1982; Deacon 1995). At the higher elevation of Cave 5, ~2 km from KRM, the MSA I has a single luminescence date of 137.4 ± 13.6 ka (Feathers 2002).

3 | Materials and Methodology

Four micromorphology blocks were collected from the Witness Baulk in 2020. Two blocks each were taken in columns along the western and eastern profiles (Figure 2), sampling the MSA I-bearing deposits to the north of the ongoing excavation. At the western location, KRM-20-302 (hereafter referred to as 302) includes the full vertical extent of the LBS and part of the SBLS, while the overlying KRM-20-301 (301) contains most of the remainder of the SBLS (Figure 4a). At the eastern location, KRM-20-304 (304) samples the LBS, and the overlying KRM-20-303 (303) includes the upper portion of the LBS and much of the SBLS (Figure 4b).

The blocks were prepared and processed (see Wurz et al. 2022, 7) at the University of Tübingen for the purposes of micromorphology and organic petrology. Eight thin sections were produced: two from each sample, with the upper designated "A" and the lower "B." They were ground relatively thick, ~50 μm rather than 30 μm, due to the ease with which softer materials could be inadvertently ground out while grinding harder materials. Additionally, one chip used in the production of a thin section underwent dry fine polishing (without lubricants).

The thin sections were analyzed with a petrographic microscope using plane- and cross-polarized light (PPL and XPL), using the descriptive terminology of Stoops (2021). A Bruker M4 Tornado μXRF analyzer allowed the production of elemental maps (Mentzer 2017). Analytical parameters matched those in previous KRM studies (Wurz et al. 2022, 7). Distinct microstratigraphic units (MSUs) were identified and described based on the micromorphology observations and elemental maps. The microfacies approach (Courty 2001) was used to group and interpret MSUs with similar properties.

Larger bone and shell fragments in the thin sections were analyzed using μFTIR (Berna 2017). Absorbance spectra were collected using an Agilent Technologies Cary 610 FTIR microscope with a germanium attenuated total reflectance objective. A digital reference library was used to classify the spectra, allowing the determination of whether a bone was heated, and to what temperature range (Larbey et al. 2019; Wurz et al. 2022). The presence or absence of the Phosphate High Temperature peak marked heating above or below ~600°C–700°C, respectively (Thompson et al. 2013; Stepka et al. 2022).

Spectra were also collected from shells to determine whether they were composed of calcite or aragonite. Where

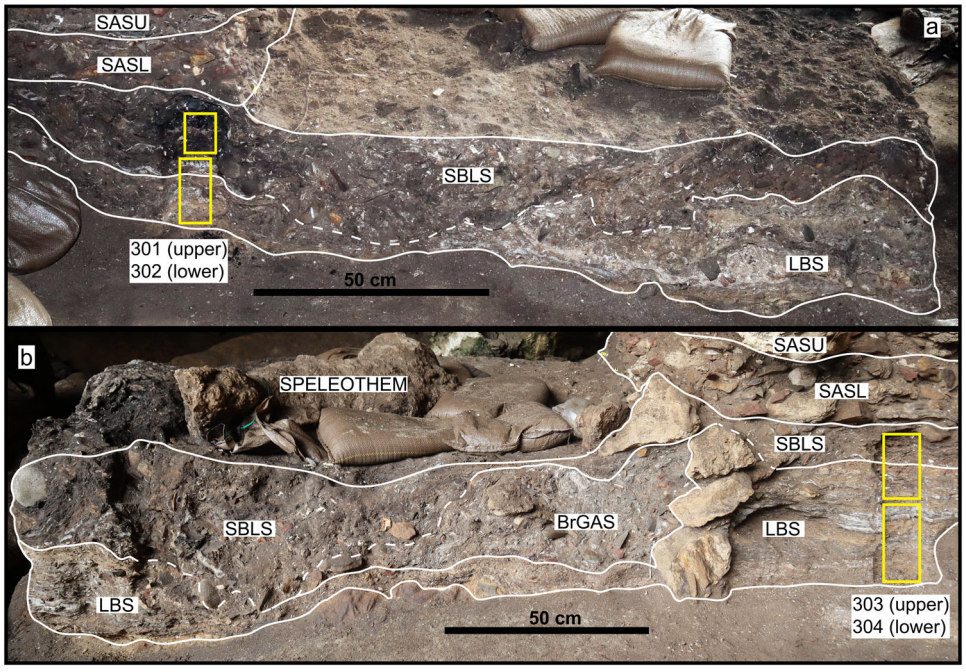


FIGURE 4 | Western (a) and eastern (b) profiles of the Witness Baulk with major stratigraphic groupings and the locations from which samples were collected for this study (photographs by K. Croll). Note the large piece of speleothem lying within the excavation, and the "rock column" between the LBS and BrGAS (a distinct unit within parts of the upper portion of the LBS) (b).

15206548, 2025, 2, Downloaded from https://onlinelibrary.wiley.com/doi/10.1002/gea.70005 by University Of Witwatersrand, Wiley Online Library on [22/10/2025]. See the Terms and Conditions (https://onlinelibrary.wiley.com/terms-and-conditions) on Wiley Online Library for rules of use; OA articles are governed by the applicable Creative Commons License

spatial relationships between the shell and burned materials and/or the petrographic properties of the fragments (Villagran 2014; Simões and Aldeias 2022) indicate that the shell was likely heated or burnt and the presence of aragonite in some or all of the fragments suggests temperatures below 400°C. If all fragments within a deposit meeting the same criteria are calcite, then they were likely heated to above 400°C, especially if multiple taxa are represented (Wurz et al. 2022; see Supporting Information), although various factors may influence the temperature at which the transformation occurs (Aldeias et al. 2019; Toffolo 2021). This approach was previously applied to combustion features at KRM (Larbey et al. 2019). Relevant results of the μFTIR analysis of the bone and shell are presented in the online Supporting Information.

The polished chip of 304 was analyzed using reflected light microscopy at a magnification of 500x. The analysis was performed following Taylor et al. (1998) under oil immersion with a Leica DMRX/MPV-SP microscope photometer in reflected white-light (RLo) and incident ultra-violet light (RUVLo) and in plane polarized (RPPLo) and cross-polarized light (RXPLo). Description and classification of the organic micro-components (macerals) were based on the nomenclature of macerals in brown coal and coal (Taylor et al. 1998; Sýkorová et al. 2005).

The determination of reflectance of plant tissues is an established means of measuring the maturation degree of organic matter in peats, brown coals, coals, and sedimentary rocks (Borrego et al. 2006). Its application in archaeology typically focuses on reconstructing the burning and preservation conditions of wood, charcoal, and char derived from bone and fats (Ligouis 2017). Reflectance analyses of charcoal, bone, and fat-derived char paired with archaeological micromorphology have been previously applied at KRM in the study of combustion features by Larbey et al. (2019) and elsewhere in South Africa (Goldberg et al. 2009; Clark and Ligouis 2010). Random reflectance in oil (mean % Rr) of the organic particles from three discrete MSUs was measured according to the standard procedure (Taylor et al. 1998). Only one measurement was made on each tissue.

4 | Results and Interpretation

4.1 | Macrostratigraphy

The western and eastern profiles of Cave 1 Witness Baulk are described below, more broadly for the entire profile, and in greater detail at two locations north of the excavation, which were subsequently sampled for micro-analysis (Figure 4).

4.1.1 | Western Profile

The LBS Member is thickest on the southern end, where it is initially dominated by sandy sediments with thin lenses of anthropogenic material, followed by a succession of thicker, shell-rich, ash, and charred deposits (Figure 4a). Moving north, the member is truncated, with several hollows on its surface. The upper surface is difficult to follow, with the exact location of the contact with overlying deposits often unclear. Most of the original vertical extent of the LBS has been lost in several places. The overlying deposits have been provisionally assigned to the SBLS. All are darker than the underlying LBS, but there are variations in: color, the presence or absence of internal stratification, and the density and organization of clasts. The contact with the overlying SASL Sub-member (specifically the Brown Occupational Soils or BOS) is characterized by increased clast density and size.

At the sample locations (301 and 302), a basal pale orangish-brown gritty sand with larger angular quartzite inclusions is overlain by faintly bedded darker silty sand deposits, which are fairly rich in shell and ash but do include interbedded sand. They are capped by a yellowish-brown sandy unit with an associated very thin ash layer. The transition to the SBLS is marked by a ~25-cm-wide, ~3-cm-thick, undulating ash feature with a faint dark lamina at its base. The ash is truncated at its upper surface in several locations. The SBLS here is particularly dark and clast-rich, with a moist fine silty sand matrix. Some stratification was observed, but this is indistinct, except for a laterally constrained (~10 cm wide) slightly undulating ashy deposit. The clasts include shell, faunal remains, rubified quartzite, lithics, and charcoal. Overall, they appear chaotic in arrangement, but there are localized areas with preferred orientations.

4.1.2 | Eastern Profile

The LBS Member is again characterized by basal sandy deposits, followed by layers rich in ash, charred material, and shell (Figure 4b). These deposits are more finely bedded than in the western profile and are interbedded with sandy deposits of varying thickness. A series of three rocks (quartzite and speleothem/tufa) form an almost vertical "rock column" in the profile just north of the ongoing excavation. They are separated by sediment but do directly touch in places. There is a notable truncation of the LBS deposits from near the southern end of the profile up to the "rock column." The Brownish Grey Ashy Sand (BrGAS) unit, which is part of the LBS, lies on this surface and is banked up against the southern face of the "rock column." To the north of the "rock column," the LBS was not truncated and is up to 32 cm thick. BrGAS is comparatively clast-rich, including many lithic artifacts, and contains patches of cemented ash. The clasts in some areas are chaotically arranged, but in others, they conform to the underlying morphology. The SBLS overlies the LBS (including BrGAS). The steeply dipping contact between BrGAS and the SBLS to the south (Figure 4b) is suggestive of the lateral truncation of the BrGAS. As in the western profile, the SBLS here has variable sedimentary properties across its extent. Its upper contact with BOS (SASL Sub-member) is marked by a significant increase in clast density and size.

At the sample locations (303 and 304), the basal deposit is yellowish-brown sand with some grit, which fines upward (both coarse and fine fraction) and has some thin, faint, and discontinuous darker laminae. It is overlain by a layer of very dense shell and ash. This is followed by silty brown sand and then a dark

15206548, 2025, 2, Downloaded from https://onlinelibrary.wiley.com/doi/10.1002/gea.70005 by University Of Witwatersrand, Wiley Online Library on [22/10/2025]. See the Terms and Conditions (https://onlinelibrary.wiley.com/terms-and-conditions) on Wiley Online Library for rules of use; OA articles are governed by the applicable Creative Commons License

silty layer with ash and dispersed shells. The overlying deposit is yellowish-brown sand with some silt, which contains very thin grey and pale orange laminae. Above this is a ~6-cm-thick succession of charred laminae and thicker ash deposits. This packet of deposits has a curved base, and the exposed portion is more than 50 cm wide. Its southern boundary is between the lower two rocks in the "rock column," and it appears to have been compressed by the deposition of the second rock. The remainder of the LBS consists of alternating beds and laminae of yellowish-brown sand, ash, and darker finer sediments, some of which is relatively rich in shells. Some ashy deposits are truncated laterally or show signs of distortion. Microfauna remains are clearly visible in the profile, unlike the lower portion of the LBS in the sample location. The transition to the SBLS is marked by darker and finer sands with some laminae of different shades, including what looks like charred material. Microfauna remains are still common, but macroscopically distinguishable ash deposits are absent. Clasts are comparatively rare and mostly small, in contrast to much of the SBLS. There are a few locations where the LBS appears to have been eroded, with darker SBLS sediments filling the spaces.

4.2 | Microstratigraphy

The two samples (302 and 301) from the western location contained a total of 29 distinct MSUs (Figures 5 and 6), while those from the eastern location (304 and 303) comprised 46 (Figures 7 and 8). MSUs are grouped into 12 MF types, which are described below. Representative photomicrographs of each MF type are provided in Figures 9–11. Foraminifera (Figure 12a) are common

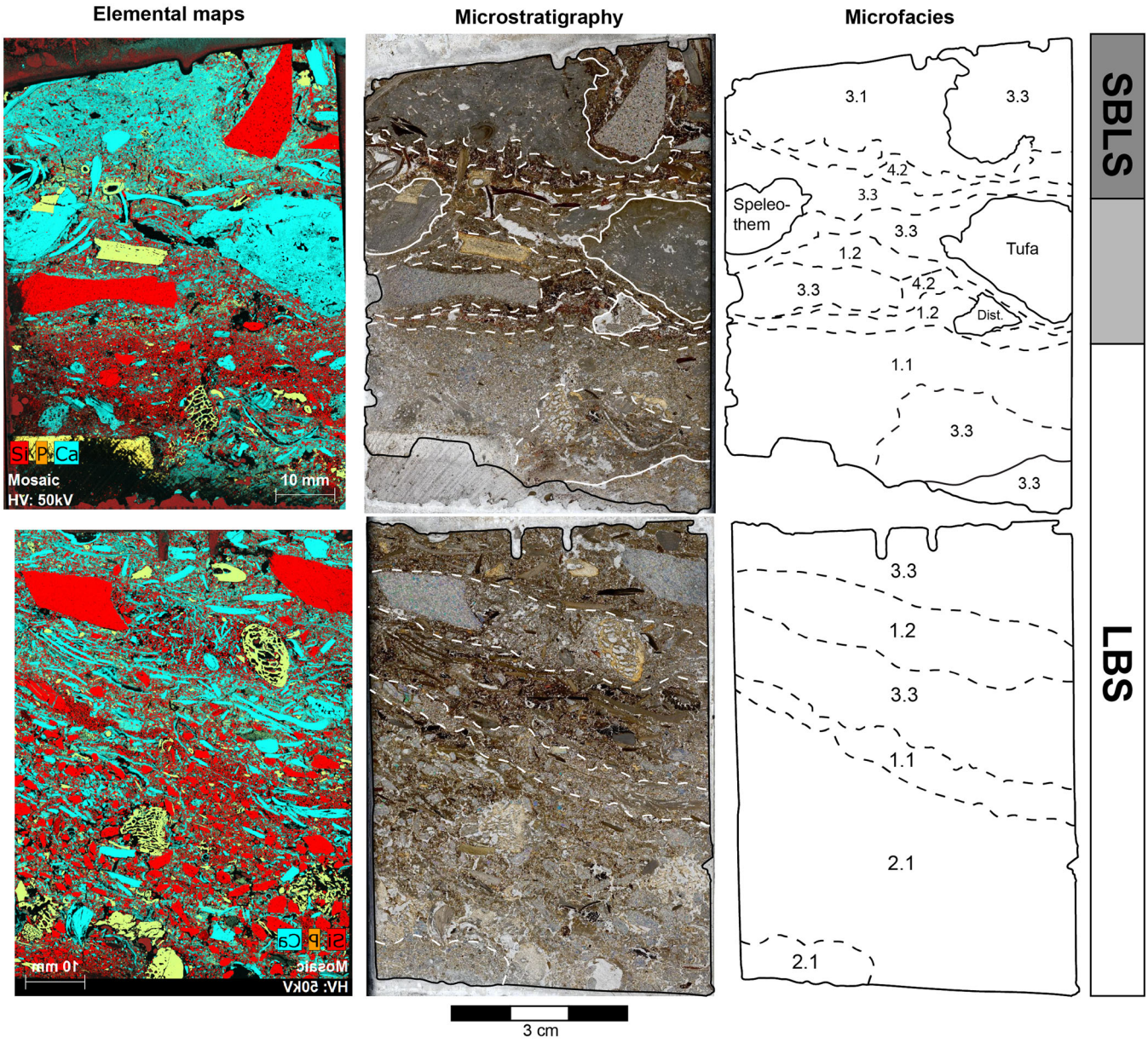


FIGURE 5 | μXRF elemental maps, microstratigraphy, microfacies attributions, and macrostratigraphy for slides A (top row) and B (bottom row) from KRM-20-302, lower half of the western sample column. On the elemental maps, blue denotes calcium (mostly ash or shell) and red represents silicon in the form of quartz and quartzite. Yellow shades show the presence of both calcium and phosphorus, for example, in bone, phosphatized ash, and apatite nodules. The paler grey portion of the stratigraphic column denotes MSUs which cannot be confidently attributed to either the LBS or SBLS.

15206548, 2025, 2, Downloaded from https://onlinelibrary.wiley.com/doi/10.1002/gea.70005 by University Of Witwatersrand, Wiley Online Library on [22/10/2025]. See the Terms and Conditions (https://onlinelibrary.wiley.com/terms-and-conditions) on Wiley Online Library for rules of use; OA articles are governed by the applicable Creative Commons License

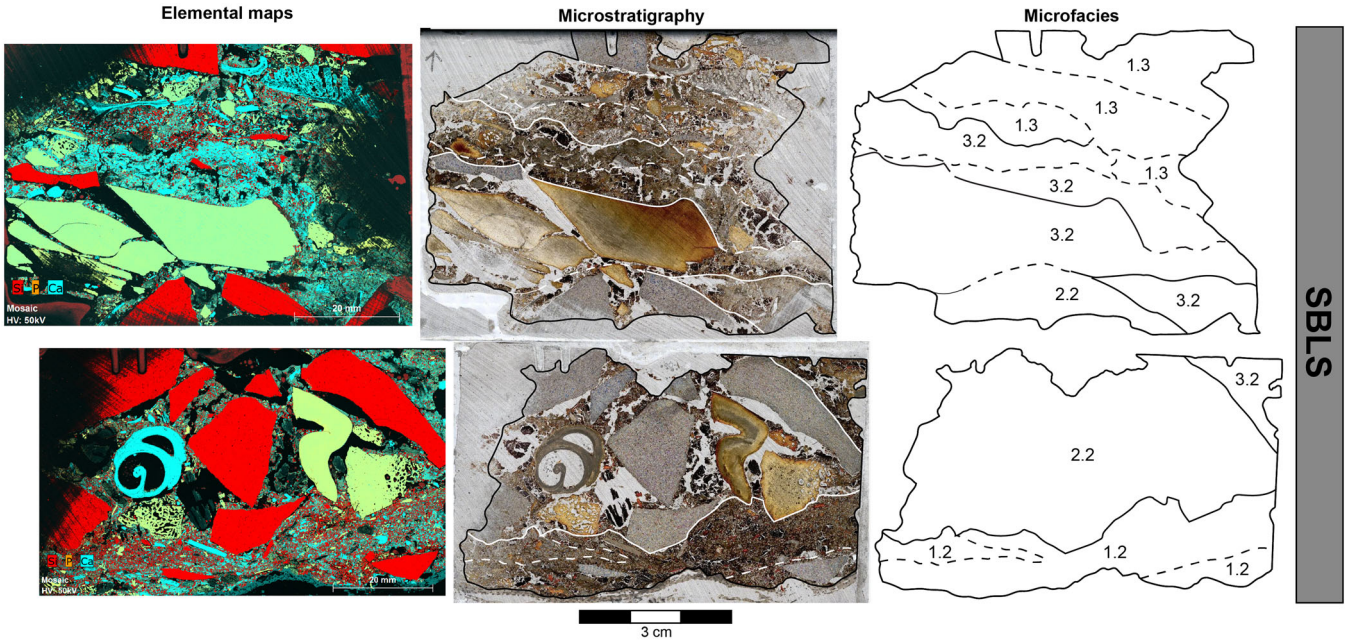


FIGURE 6 | μXRF elemental maps, microstratigraphy, microfacies attributions, and macrostratigraphy for slides A (top row) and B (bottom row) from KRM-20-301, upper half of the western sample column. On the elemental maps, blue denotes calcium (mostly ash or shell) and red represents silicon in the form of quartz and quartzite. Yellow shades show the presence of both calcium and phosphorus, for example, in bone, phosphatized ash, and apatite nodules.

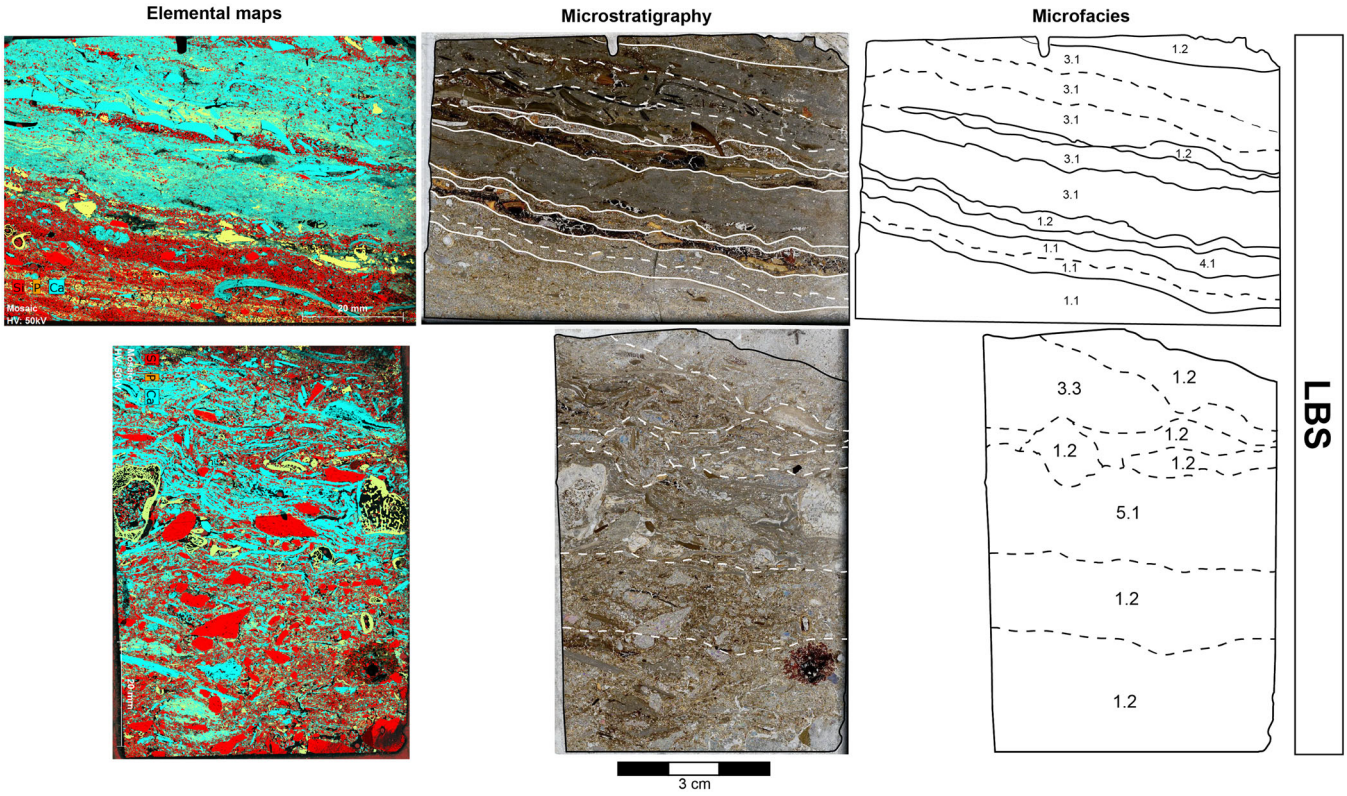


FIGURE 7 | μXRF elemental maps, microstratigraphy, microfacies attributions, and macrostratigraphy for slides A (top row) and B (bottom row) from KRM-20-304, lower half of the eastern sample column. On the elemental maps, blue denotes calcium (mostly ash or shell) and red represents silicon in the form of quartz and quartzite. Yellow shades show the presence of both calcium and phosphorus, for example, in bone, phosphatized ash, and apatite nodules.

15206548, 2025, 2, Downloaded from https://onlinelibrary.wiley.com/doi/10.1002/gea.70005 by University Of Witwatersrand, Wiley Online Library on [22/10/2025]. See the Terms and Conditions (https://onlinelibrary.wiley.com/terms-and-conditions) on Wiley Online Library for rules of use; OA articles are governed by the applicable Creative Commons License

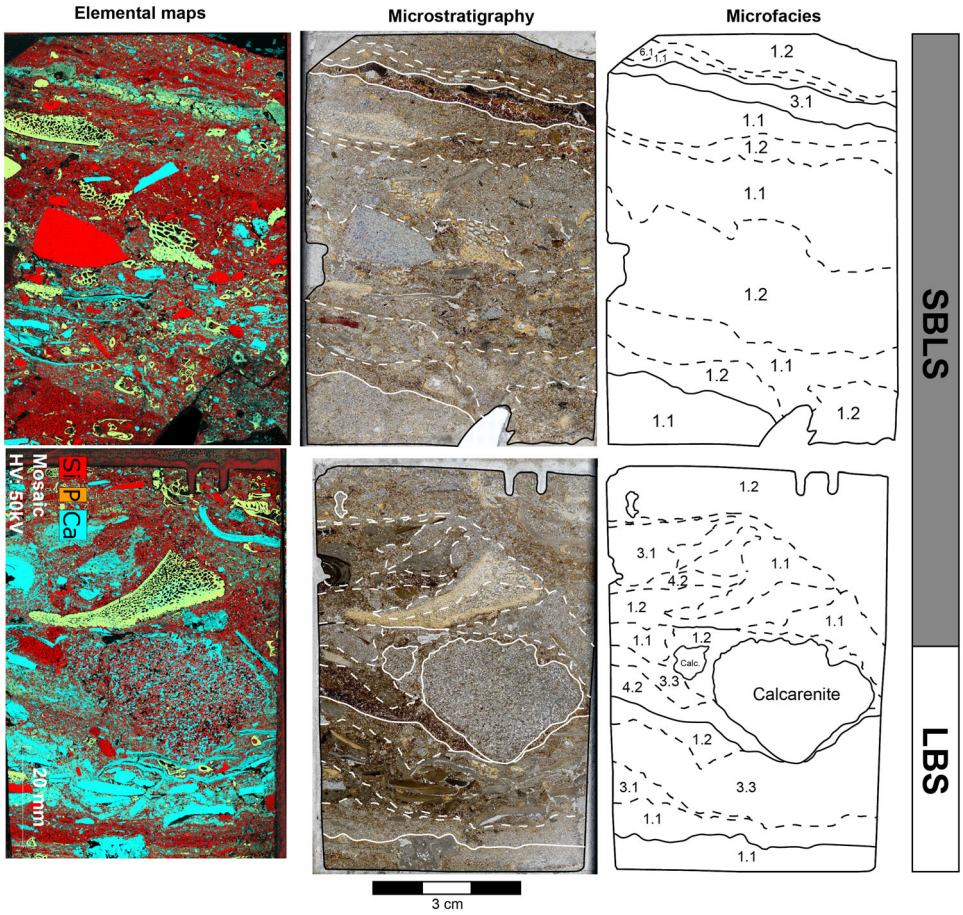


FIGURE 8 | μXRF elemental maps, microstratigraphy, microfacies attributions, and macrostratigraphy for slides A (top row) and B (bottom row) from KRM-20-303, upper half of the eastern sample column. On the elemental maps, blue denotes calcium (mostly ash or shell) and red represents silicon in the form of quartz and quartzite. Yellow shades show the presence of both calcium and phosphorus, for example, in bone or teeth, phosphatized ash, and apatite nodules.

in many MSUs. The microstratigraphy and the relationship between the MSUs and the LBS and SBLS members are described in the online Supporting Information.

4.2.1 | MF 1.1 Shelly Sand (Slides 302A&B, 303A&B, 304A)

This MF type comprises quartz sand (sub-angular to sub-rounded) and some sand-sized shells with a limited fine matrix (Figure 9a,b). The matrix is predominantly wood ash, which is almost entirely altered to apatite, but siliceous silt and clay fill interstitial spaces in places. The sand is interbedded with predominantly phosphatized ash (or ash-rich) lenses in a few cases, and ashy patches occur. Rounded ash aggregates and aggregates of calcareous mud appear in some deposits. Angular and more rounded shell fragments are present at a low frequency; few are > 5 mm. Bone is typically less common and ranges from sand-sized to several centimeters. However, some deposits are rich in bone (including microfauna). Only a single partial tooth (microfauna) was observed, in slide 303B. Some in situ fragmentation of shell and bone occurred. Quartzite fragments < 1 cm are present in all MSUs but are never a significant component. Foraminifera are common but are only present within pockets of the fine matrix or occasionally as distinct lenses comprised of only foraminifera.

4.2.2 | MF 1.2 Ashy Shelly Sand (Slides 301B, 302A&B, 303A&B, 304A&B)

This MF type is characterized by shelly quartz sand in an ashy matrix (Figure 9c,d). The quartz is sub-angular to sub-rounded, while the shell (far less common than the quartz) is more rounded. The matrix is primarily recrystallized ash, with less common secondary calcite. There is also fine comminuted organic material and some siliceous silt and clay (usually far less than the organics), making the matrix appear relatively dark, but the proportion and distribution of these materials vary widely. The degree to which the matrix fills the interstitial space is also variable. Phosphatization of the matrix is minor and patchy but is widespread. Many MSUs contain patches or lenses of comparatively pure ash, which are often more strongly phosphatized than the matrix (Figure 13d). Small bone fragments (coarse sand-sized to ~2 mm) are common. Similarly sized apatite nodules and guano fragments are very rare. Coarser inclusions occur at different densities and include shell fragments, larger bone fragments (up to ~3 cm), microfauna remains, and quartzite (including artifacts). Almost all teeth (all microfauna) observed in the thin sections were from this MF type and were found in slides 303A and B only. The

15206548, 2025, 2, Downloaded from https://onlinelibrary.wiley.com/doi/10.1002/gea.70005 by University Of Witwatersrand, Wiley Online Library on [22/10/2025]. See the Terms and Conditions (https://onlinelibrary.wiley.com/terms-and-conditions) on Wiley Online Library for rules of use; OA articles are governed by the applicable Creative Commons License

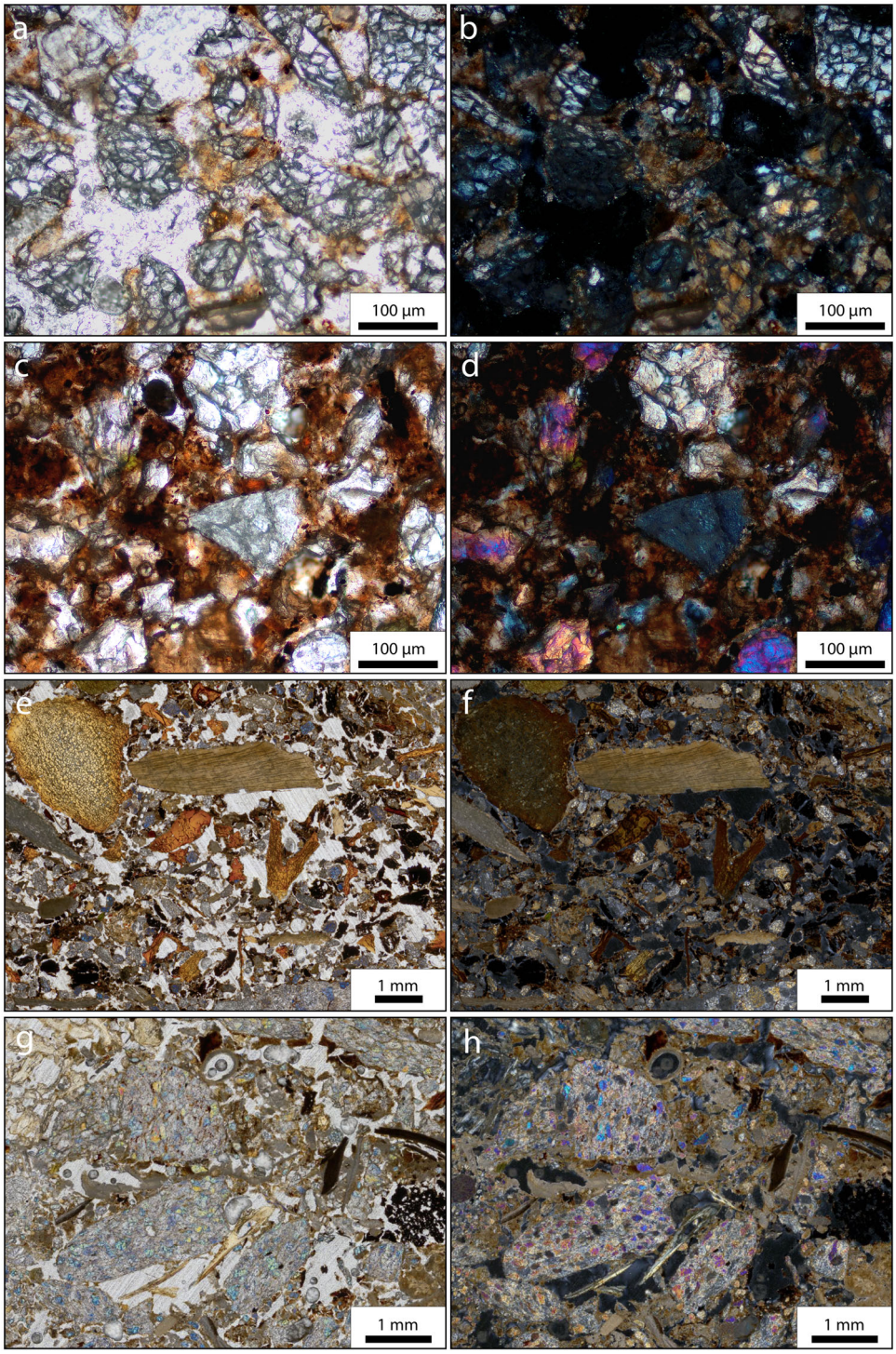


FIGURE 9 | Representative photomicrographs of microfacies. Note that due to the relative thickness of the slides, some of the components in this and subsequent figures do not look exactly as they would in a thin section of standard thickness. (a) Shelly sand with a limited phosphatic matrix (MF 1.1), PPL. Note the clear dominance of quartz grains over the shell. (b) Same view, XPL. (c) Shelly sand with an ashy slightly phosphatized matrix (MF 1.2), PPL. (d) Same view, XPL. (e) Loose heterogenous mix of sand, charcoal, and bone (MF 1.3), PPL. (f) Same view, XPL. (g) Fine quartzite gravel and sand in a calcareous (mainly ash) matrix (MF 2.1), PPL. (h) Same view, XPL.

quartzite fragments are typically angular and range from coarse sand-sized to ~2 cm. Charcoal is relatively common in a few deposits. In situ breakage of faunal remains and shell is absent in most MSUs and typically rare. Foraminifera are present in all deposits.

4.2.3 | MF 1.3 Loose Coarse Heterogenous Sand (Slide 301A)

This MF type is made up of a loose, chaotic combination of shelly sand, angular bone and shell fragments, and charcoal

15206548, 2025, 2, Downloaded from https://onlinelibrary.wiley.com/doi/10.1002/gea.70005 by University Of Witwatersrand, Wiley Online Library on [22/10/2025]. See the Terms and Conditions (https://onlinelibrary.wiley.com/terms-and-conditions) on Wiley Online Library for rules of use; OA articles are governed by the applicable Creative Commons License

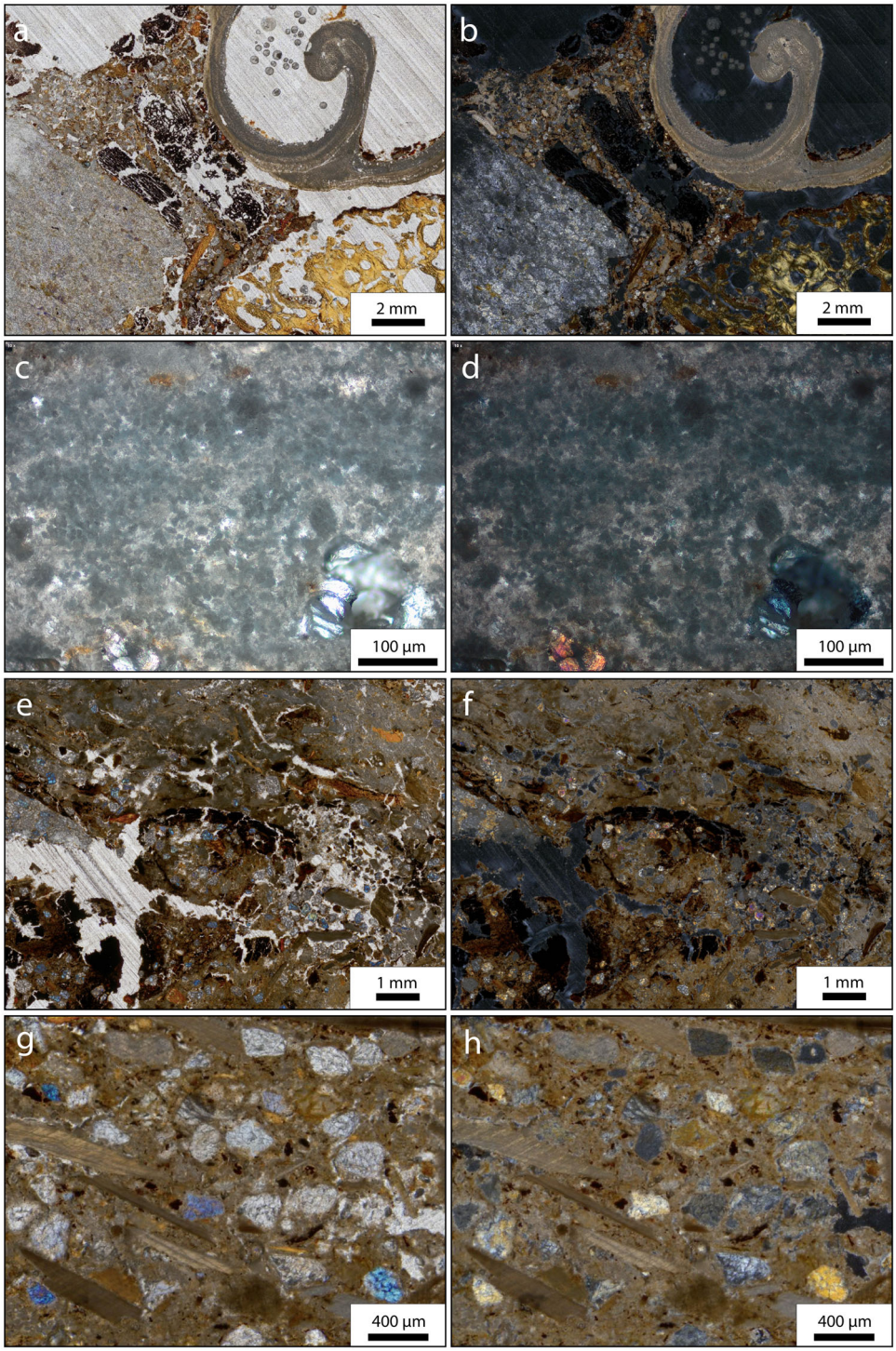


FIGURE 10 | Representative photomicrographs of microfacies. (a) Heterogeneous clasts with the blocky matrix of wood ash and various small inclusions (MF 2.2), PPL. (b) Same view, XPL. (c) Partly recrystallized wood ash (MF 3.1), PPL. Note the darker ash rhombs and lighter recrystallized ash. (d) Same view, XPL. (e) Wood ash with sand and anthropogenic inclusions (MF 3.2), PPL. Note the filled chamber and undulating charred lenses. (f) Same view, XPL. (g) Sandy ash with coarse inclusions (MF 3.3), PPL. (h) Same view, XPL.

fragments (Figure 9e,f). The various fragments range from coarse sand to ~1 cm. There is notable variation in the proportions of these materials, with some domains dominated by one material and others far more mixed. Secondary calcite coats many grains, and there are some sand-sized aggregates of recrystallized wood ash and finely comminuted organic material. Some areas have a denser matrix of recrystallized and cemented wood ash, secondary calcite, and fine organic material. The calcareous matrix has undergone very limited phosphatization by secondary apatite, and some shells have been slightly dissolved. The charcoal contains some secondary calcite and apatite, and some bone fragments have been slightly calcified. Larger clasts (> 1 cm), including shell, bone, and lithics, are typically oriented more horizontally and/or

15206548, 2025, 2, Downloaded from https://onlinelibrary.wiley.com/doi/10.1002/gea.70005 by University Of Witwatersrand, Wiley Online Library on [22/10/2025]. See the Terms and Conditions (https://onlinelibrary.wiley.com/terms-and-conditions) on Wiley Online Library for rules of use; OA articles are governed by the applicable Creative Commons License

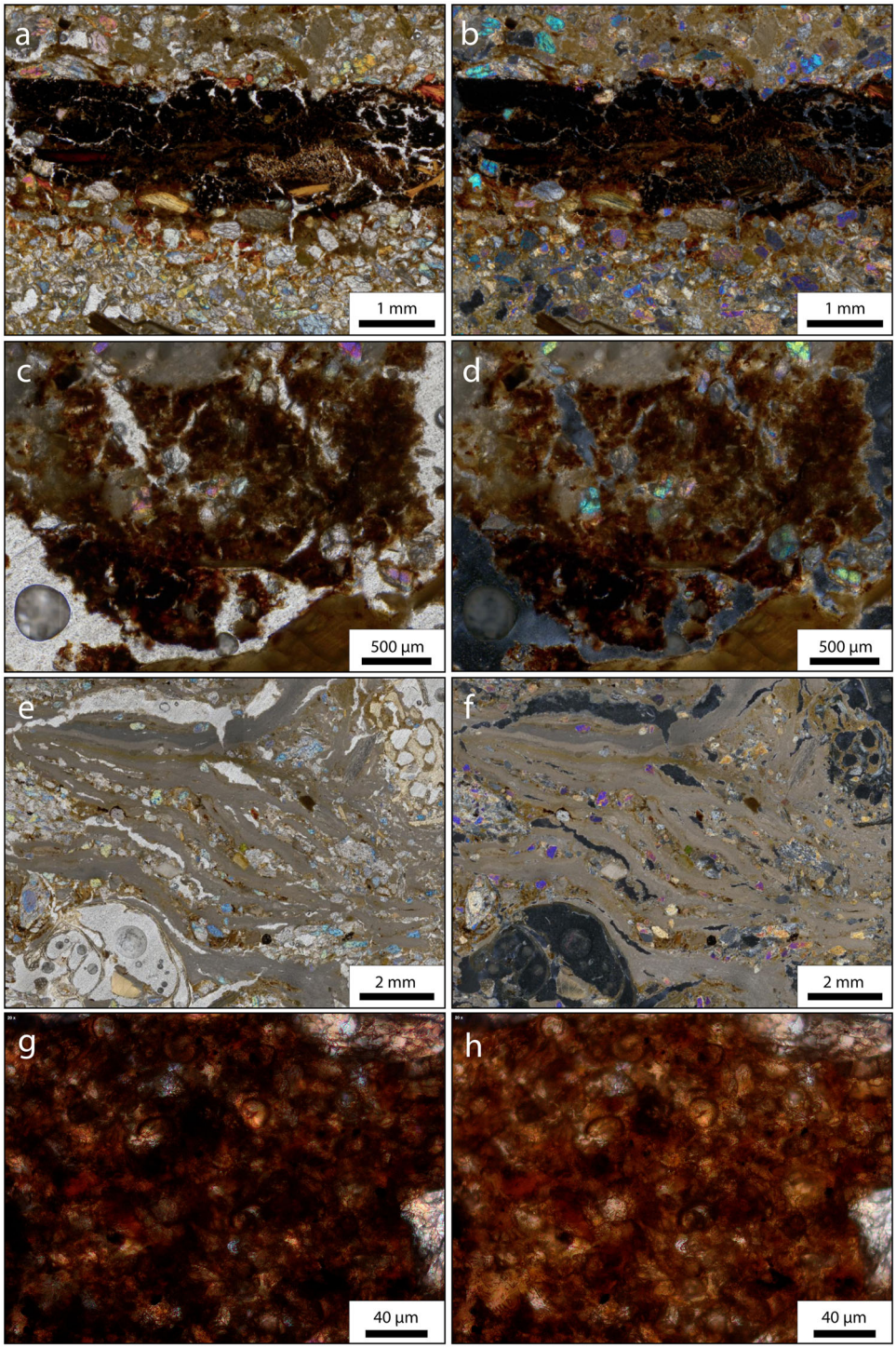


FIGURE 11 | Representative photomicrographs of microfacies. (a) Charred organic material in an ashy matrix with both burnt and unburnt bone (MF 4.1) sandwiched between two sandy deposits, PPL. (b) Same view, XPL. (c) Fine charred organic material in an ashy matrix (MF 4.2), PPL. (d) Same view, XPL. (e) Densely packed shell in the matrix of ash and secondary calcite (MF 5.1), PPL. (f) Same view, XPL. (g) Iron-rich siliceous silt and clay with foraminifera and rare sand grains (MF 6.1), PPL. (h) Same view, XPL.

correspond to the general deposit morphology. Several larger bones analyzed with µFTIR were not heated above 600°C, but the smaller fragments have a range of colors, suggesting potential differential heating. Most bone and shell fragmentation appears to have occurred before deposition. In situ fragmentation of charcoal is more common. Foraminifera are extremely rare.

4.2.4 | MF 2.1 Fine Quartzite Gravel (Slide 302B)

This MF type comprises sub-rounded to angular, mostly elongated quartzite ranging from very coarse sand-sized up to ~6 mm, and shell fragments of similar size and shape, in a matrix of shelly sand and fine calcite (Figure 9g,h). In situ fragmentation is very rare. There is localized

15206548, 2025, 2, Downloaded from https://onlinelibrary.wiley.com/doi/10.1002/gea.70005 by University Of Witwatersrand, Wiley Online Library on [22/10/2025]. See the Terms and Conditions (https://onlinelibrary.wiley.com/terms-and-conditions) on Wiley Online Library for rules of use; OA articles are governed by the applicable Creative Commons License

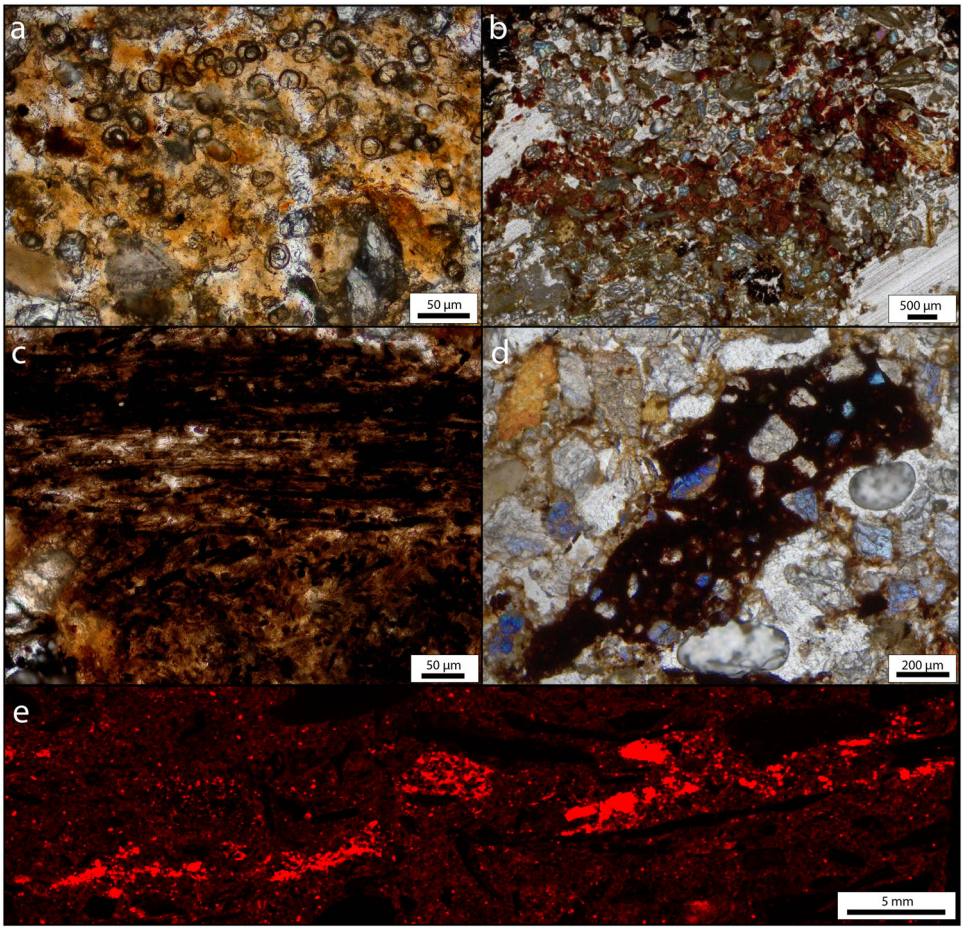


FIGURE 12 | (a) Unidentified foraminifera in a phosphatized ashy matrix, PPL. (b) Deformed apatite crust in ashy sand of MF 1.2 (302 A), PPL. (c) Unburnt organic material in MF 4.2, PPL. (d) Sub-angular iron-rich aggregate with fine quartz sand inclusions, PPL. (e) µXRF map of iron distribution showing the discontinuous lens of iron-rich aggregates in 303A. This scan was made on the chip.

variation in the proportion of shell and fine calcite. The fine calcite includes recrystallized ash and secondary calcite. There is some phosphatization of the calcite and rare dissolution of the shell. Very small apatite nodules and localized very thin crusts are present but uncommon. Bone up to ~1 cm largely comprises a few whole pieces, but there are smaller scattered fragments (mostly fairly angular), with some in-situ fragmentation. Limited calcification of the bone was noted. Both fine charred organic material and small pieces of charcoal are scattered throughout at low density. Foraminifera are uncommon.

4.2.5 | MF 2.2 Coarse Heterogeneous Gravel (Slides 301A&B)

This deposit contains a mix of different types of relatively large clasts (from ~6 mm to ~3 cm) including angular quartzite (some lithic artifacts), whole shell, bone, and charcoal (Figure 10a,b). The clasts display a range of orientations, from almost horizontal to near vertical. The matrix is recrystallized ash rich in finely comminuted organic material with shelly quartz sand and sand-sized to ~3 mm angular bone and shell fragments. The deposit is locally clast-supported but matrix-supported overall. The matrix occasionally has a sub-angular blocky microstructure. No in situ breakage of bone or shell is visible, and potential in situ breakage of charcoal is limited to the upper portion of the deposit. There is minor patchy phosphatization of the matrix, and the charcoal fragments contain some secondary calcite and apatite. More porous bone has been slightly calcified. Some foraminifera are present in the matrix.

4.2.6 | MF 3.1 Ash (Slides 302A, 303A&B, 304A)

This MF type comprises wood ash with anthropogenic inclusions and rare sand-sized quartz (Figure 10c,d). Where present, sand often forms extremely thin lines within the ash. Otherwise, it is distributed at extremely low density. Recrystallization of ash is fairly common but not complete, with thin bands of greater recrystallization. Phosphatization is widely observed but varies in intensity and distribution. Patches are most common, but there are also sub-millimeter lenses. In some very thin MSUs, calcite has been almost completely replaced by apatite. Channels are present in most units, at varying densities.

15206548, 2025, 2, Downloaded from https://onlinelibrary.wiley.com/doi/10.1002/gea.70005 by University Of Witwatersrand, Wiley Online Library on [22/10/2025]. See the Terms and Conditions (https://onlinelibrary.wiley.com/terms-and-conditions) on Wiley Online Library for rules of use; OA articles are governed by the applicable Creative Commons License

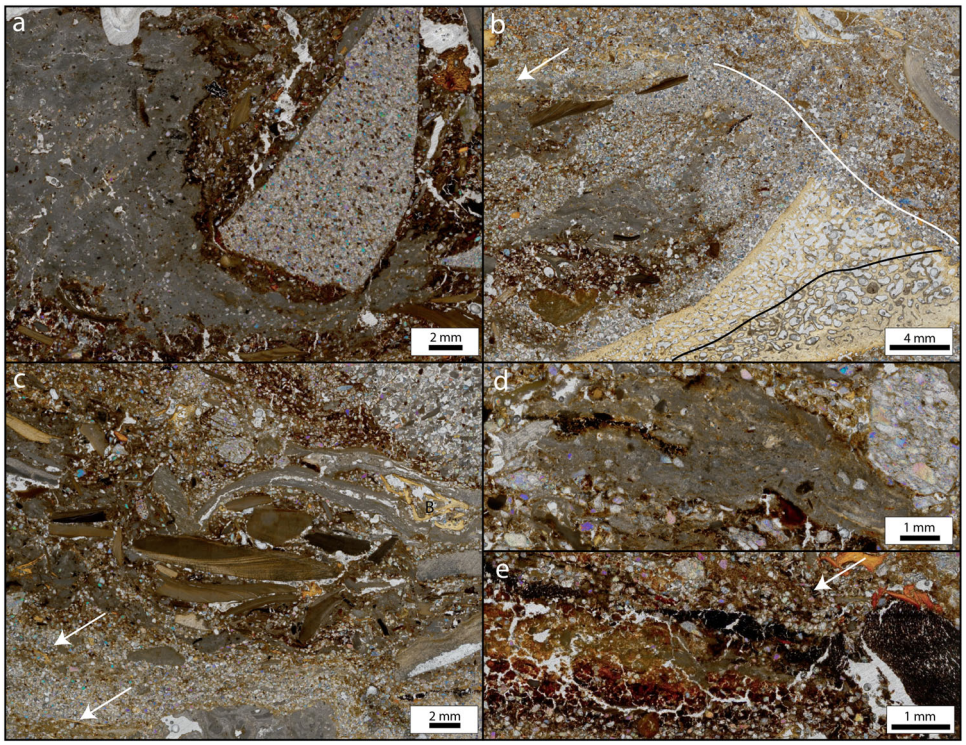


FIGURE 13 | (a) Truncated hearth with possible soft sediment deformation at the base of the SBLS in the western profile, PPL. (b) Truncated hearth in the upper LBS, eastern profile, PPL. The white line marks an erosional contact with the infilling SBLS. Note the relatively low proportion of the calcareous matrix in the SBLS, both in the infill and above the hearth. The black line indicates the extent of secondary calcification (below the line) and subsequent decalcification (above the line) in an unburnt bone. The white arrow shows the location of a sub-millimeter lens of foraminifera in the MF 1.1 sands above the hearth. (c) Compressed (by trampling) anthropogenic or anthropogenic-component-rich deposits in the LBS, eastern profile, PPL. Note the loss of stratigraphic resolution and the crushed unburnt bone fragment (B). Some shell fragments are composed of calcite and others of aragonite. The white arrows indicate thin lenses of (mostly) phosphatized ash within the otherwise largely decalcified MF 1.1 sands below. (d) Remains of a combustion feature in the basal gritty sand, eastern profile, PPL. (e) Heavily phosphatized hearth in the upper SBLS, eastern profile, PPL. Note the dissolution of the ash associated with the upper charred layer. The white arrow marks part of the deposit of iron-rich silt and clay (MF 6.1) near the contact with the SASL sub-member.

4.2.7 | MF 3.2 Ash With Coarse Inclusions (Slides 301A&B)

This MF type is characterized by ash with anthropogenic inclusions and some shelly sand (Figure 10e,f). Recrystallization is patchy, with some distinct bands of recrystallized ash, most notably near the top of MSUs. Some secondary calcite is present, particularly in bone fragments. Fine charred material is distributed throughout. Coarser inclusions are more common and diverse than in MF 3.1. These include shell, bone, charcoal, and lithics, with notable variations in their proportions and sizes. Larger inclusions (> 5 mm) are typically relatively horizontal or conform to the underlying morphology, but there are some zones with a more chaotic fabric. Thin lenses of charcoal (often articulated) are common. These typically undulate and are sometimes associated with planar voids. There is some in situ fragmentation of bone and shell, but this seems to have mostly occurred ex situ as few associated fragments appear to re-fit. Phosphatization is variable in extent. Many phosphatized lenses are pseudomorphic to thin charred lenses, with some unaltered charred material remaining. There are rare examples of small coprolites and rounded aggregates of phosphatized ash. Channels up to ~3 mm wide are relatively common. Some are filled or partially filled with loose sand and reworked anthropogenic materials. Accommodated or partially accommodated planar voids are common in some MSUs.

4.2.8 | MF 3.3 Sandy Ash (Slides 302A&B, 303B, 304B)

This MF type comprises an ash matrix with a significant (but variable) proportion of shelly sand (Figure 10g,h). Recrystallization of ash is very common, and there is some secondary calcite. Fine charred organic material is distributed throughout the matrix, with particularly high concentrations making the calcareous material appear 'dirty'. Phosphatization is variable in distribution and intensity. Shell fragments are present in all deposits but vary considerably in size and frequency. Bone (mostly fragmentary), quartzite (including lithics), and charcoal are found in some MSUs.

4.2.9 | MF 4.1 Charred (Slide 304A)

This deposit is a dense concentration of charcoal and fine charred organic material, with ash filling most interstitial space (Figure 11a,b). There is some minor phosphatization. Bone fragments ranging from very coarse sand to ~9 mm are numerous. The μFTIR spectra indicate a range of temperatures, with some unburnt

15206548, 2025, 2, Downloaded from https://onlinelibrary.wiley.com/doi/10.1002/gea.70005 by University Of Witwatersrand, Wiley Online Library on [22/10/2025]. See the Terms and Conditions (https://onlinelibrary.wiley.com/terms-and-conditions) on Wiley Online Library for rules of use; OA articles are governed by the applicable Creative Commons License

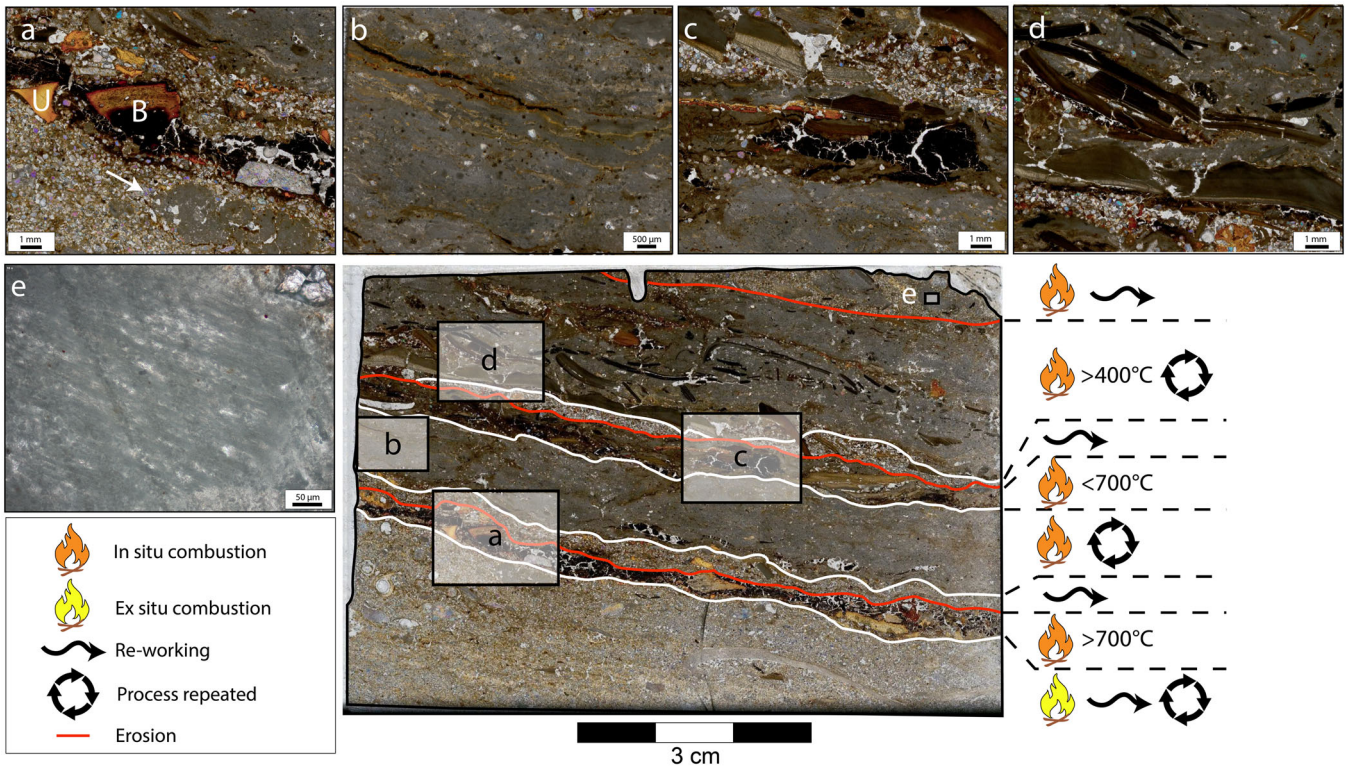


FIGURE 14 | Summary of the anthropogenic processes involved in forming the deposits in slide 304A, LBS, eastern profile. All insets are in PPL. (a) Largely intact basal charred layer underlain by MF 1.1 and overlain by MF 1.2. Note the close association of burnt (B) and unburnt (U) bone fragments. No bone in the MF 1.2 deposit was found to be burnt. The white arrow shows a rounded ash aggregate beneath the hearth. (b) Alternating laminae of ash, recrystallized ash, phosphatized ash, and (less commonly) charred material. Sand grains are distributed throughout at very low density but sometimes form discontinuous lines of one or two grains in thickness. (c) Discontinuous charred material with burnt bone and both calcite and aragonite shell fragments (the latter are not pictured) in ash of MF 3.1. Note the unconformable contact with the overlying sand. (d) Burnt shell of multiple taxa, which were all found to be composed of calcite, indicating a minimum temperature of 400°C. (e) Articulated wood ash or calcified charcoal in ash, which has undergone limited reworking at the top of the hearth stack.

fragments, some burnt below 700°C, and others at more than 700°C. Organic petrology (see the online Supporting Information) reveals the presence of fat-derived char, supports the observation that charcoal has been altered (see Figure 14), and demonstrates that charcoal formation occurred at 280°C.

4.2.10 | MF 4.2 Fine Charred (Slides 302A, 303B)

These deposits are made up of concentrated fine charred organic material in an ashy matrix with occasional small charcoal pieces (Figure 11c,d). Shell fragments and quartz sand are present, with the former ranging up to ~9 mm. Bone is uncommon and mostly comprises angular fragments < 2 mm. Rare unburnt organic material was observed in some MSUs. Localized phosphatization of ash occurs.

4.2.11 | MF 5.1 Dense Shell (Slide 304B)

This deposit comprises a very densely packed shell in a matrix of shelly sand and fine calcite (recrystallized ash with some secondary calcite) (Figure 11e,f). The shell is typically horizontal, with localized more steeply dipping occurrences due to the presence of harder inclusions. Fine charred organic material is present at low densities within the ash, and charcoal is uncommon. Larger inclusions include quartzite clasts up to ~1.2 cm and bone up to ~1.5 cm. Angular quartzite fragments appear to be lithic debitage. There is some in-situ fragmentation of shell and bone, with limited fragment movement. Both dissolution and compression of the shell are commonly observed, with delamination less common. Phosphatization was observed in a few shells. Minor secondary calcification of bone was noted. Foraminifera occur in the calcareous matrix and sandier domains.

4.2.12 | MF 6.1 Fine Siliceous Sediment (Slide 303A)

This deposit is primarily siliceous and relatively iron-rich silt and clay, with some quartz sand (Figure 11g,h). Sand is scattered throughout, but there are some concentrations. Other sand-size or larger inclusions are very rare. There is no phosphate, and calcite is absent except in the form of numerous foraminifera.

4.3 | Microfacies Interpretation

The formation of each of the MF types is discussed here.

15206548, 2025, 2, Downloaded from https://onlinelibrary.wiley.com/doi/10.1002/gea.70005 by University Of Witwatersrand, Wiley Online Library on [22/10/2025]. See the Terms and Conditions (https://onlinelibrary.wiley.com/terms-and-conditions) on Wiley Online Library for rules of use; OA articles are governed by the applicable Creative Commons License

4.3.1 | Shelly Sand

Shelly sand is present in many of the MF types and is the dominant component in three MFs: 1.1, 1.2, and 1.3. It was introduced into the site by either aeolian or colluvial processes from two possible sources: beach and/or dune deposits seaward of the site complex and the aeolianites above KRM (Deacon and Geleijnse 1988). Sand- to pebble-sized angular fragments of quartzite occur in most MFs, most notably in the sandy MFs. Some are lithic debitage, but many derive from host rock breakdown due to salt weathering and insolation (Butzer 1982; Deacon and Geleijnse 1988; Morrissey et al. 2023).

The sandy MFs are divided based on the proportion of anthropogenic materials (including ash, charred organic material, and bone and shell fragments) within the sand. Here, they are discussed in a progression from least to most altered by post-depositional processes.

The composition and structure of MF 1.3 are consistent with the reported properties of experimental and archaeological deposits formed by dumping material removed from hearths and adjacent or underlying sediment during hearth maintenance (e.g., Schiegl et al. 2003; Miller et al. 2010, 2013; Marcazzan et al. 2022). The aggregates of recrystallized ashy sand could be rip-up clasts produced during sweeping (Miller et al. 2010). The high proportion of bone fragments broken ex situ supports the interpretation that the material was swept, but some breakage likely occurred due to trampling before hearth maintenance. The almost complete lack of trampling after dumping is an important factor in the preservation of these deposits (Miller et al. 2013; Rentzel et al. 2017). The occurrence of multiple dumping events is also supported by the orientation of the larger clasts, which suggests that they were discarded onto surfaces between dumping events.

The ashy shelly sand of MF 1.2 was initially like MF 1.3 in having been swept or raked from in and around hearths (Miller et al. 2010, 2013). However, this material was subsequently reworked and mixed with otherwise geogenic sands through trampling and other physical disturbances (Miller et al. 2013; Rentzel et al. 2017). There is a comparatively high proportion of ashy matrix (both phosphatized and not) in the sand, although this does vary. The re-precipitation of secondary apatite as a result of the breakdown of guano caused the phosphatization of ash (Karkanas et al. 2000). This process can lower pH levels in the sediment, resulting in the dissolution of calcite, including wood ash (Schiegl et al. 1996; Karkanas 2017). The differing proportions of ash in some deposits may reflect variations in anthropogenic input, but it is likely that some ash has been dissolved and that the phosphatization of ash aided preservation to some extent (Karkanas et al. 2000). Both birds and bats could have contributed guano.

MF 1.1 deposits are more geogenic in character and are poor in ashy matrix relative to MF 1.2. The comparatively limited sand-sized shells, the partial dissolution of most large shell fragments and ash aggregates, and the general scarcity of non-phosphatized ash all indicate varying degrees of incomplete decalcification (Goldberg 2000). A lower frequency of small bone fragments suggests that many of these deposits may have initially contained less reworked anthropogenic material than the MF 1.2 deposits, meaning that the difference in the amount of ash between these MF types may not only be due to dissolution. The presence of ash-rich lenses (mostly phosphatized) may be a result of periods of better preservation of the matrix or of more intensive periods of human activity on the site.

4.3.2 | Gravel

MF 2.1 is broadly similar to MF 1.2 and was likely formed by the same general processes (reworking of anthropogenic materials into geogenic sediments). However, abundant autogenic quartzite suggests either a far more rapid breakdown of the host rock, reduced input of allogenic sand, or a combination of these (Morrissey et al. 2023). The relatively limited matrix could reflect greater dissolution of non-phosphatized ash or less availability of anthropogenic material.

The chaotic fabric of MF 2.2 (Figure 6) and the mix of large anthropogenic components are consistent with dumping (Miller et al. 2010) but also with colluvial reworking (Mentzer 2014). However, the absence of rounded aggregates, the presence of relatively angular charcoal fragments (although these have not survived well in the thin section due to challenges during processing), and the excellent preservation of whole shells in close association with lithics all support dumping as the depositional process (Goldberg 2003; Mentzer 2014; Mallol et al. 2017). The properties of the limited matrix suggest sweeping of combustion materials and associated shelly sand (Miller et al. 2010). The deposit is matrix-supported, suggesting that the matrix and clasts were deposited in one event, rather than the finer sediment filtering into the deposit after the initial dumping. MF 2.2 appears to be the product of site maintenance activities carried out around a hearth with a focus on removing larger clasts as well as sweeping away ash and other materials from the hearth and its periphery.

4.3.3 | Ash

The ash in these three MF types is consistent with the complete combustion of wood (Canti and Brochier 2017). MF 3.1 is characteristic of in situ (generally) undisturbed hearths (Mentzer 2014; Mallol et al. 2017). The incomplete recrystallization of ash is the result of the movement of water through the ash (Karkanas et al. 2007; Karkanas 2021), with secondary calcite potentially introduced by dripwater (Deacon and Geleijnse 1988). The phosphatization of ash is by secondary apatite leached from guano (Karkanas et al. 2000; Karkanas 2017). The distinct laminae of phosphatized or recrystallized ash reflect periods of surface exposure (Morrissey et al. 2023, fig. 19). Small channels indicate limited bioturbation by burrowing mesofauna (Stoops 2021).

The presence of numerous charred laminae within the ash of MF 3.2, and the relatively limited input of geogenic clastic material, indicates that these MSUs are in situ hearths (Mentzer 2014; Mallol et al. 2017). In-situ fragmentation of bone and shell and the undulating charred laminae suggest trampling (Rentzel et al. 2017). Although generally relatively minor, this has impacted the integrity of distinct layers and potentially introduced additional sand into the ash. Bioturbation by mesofauna also occurred and a combination of the burrowing and

15206548, 2025, 2, Downloaded from https://onlinelibrary.wiley.com/doi/10.1002/gea.70005 by University Of Witwatersrand, Wiley Online Library on [22/10/2025]. See the Terms and Conditions (https://onlinelibrary.wiley.com/terms-and-conditions) on Wiley Online Library for rules of use; OA articles are governed by the applicable Creative Commons License

infilling of chambers resulted in some loss of stratigraphic integrity, but this is relatively minor in comparison to some recorded cases of similar bioturbation (Mentzer 2011, 2014).

The proportion of shelly sand in MF 3.3 indicates greater geogenic input than in MFs 3.1 and 3.2. As with MF 1.2, MF 3.3 is interpreted as anthropogenic deposits reworked through processes like trampling and site maintenance (Miller et al. 2013; Mallol et al. 2017; Rentzel et al. 2017). The greater proportion of anthropogenic materials in MF 3.3 than observed in MF 1.2 might indicate greater availability of these materials due to more intensive occupation or the sampled locations being closer to the source of these materials. Alternatively, this could reflect more localized reworking, with trampling and other processes resulting in the breakage of shell and bone, the mixing of distinct anthropogenic deposits, and the introduction of geogenic sand, but with relatively limited lateral redistribution of ash and other anthropogenic components.

4.3.4 | Organic Material

The single MSU assigned to MF 4.1 can be interpreted as the base of a hearth, where the wood was not fully burnt to ash (Mallol et al. 2017). Some burnt bone fragments are likely to have been discarded into the fire. The mix of fragments with different degrees of heating in the upper portion of the deposit (some exceeding 700°C) indicates that temperatures were not uniform within the hearth. This is supported by charcoal reflectance values, which show charcoal formation at 280°C (Supporting Information S1: Figure S3). Bone fragments at the base of the deposit may have been present on the surface before the formation of the hearth (Mallol et al. 2013), and none of the analyzed fragments show evidence of heating above 500°C, suggesting limited penetration of heat into the substrate.

The fine charred organic material that dominates MF 4.2 and the association with ash-dominated deposits (MFs 3.1 and 3.3) suggests a hearth base. Two of the four MSUs assigned to this MF have been deformed and compressed, and sand is present in all four. Unburnt organic material (Figure 12c) and some charcoal fragments suggest that the fine charred organic material is the remains of incompletely burnt non-woody plant matter rather than charcoal, which has broken down through physical and/or chemical processes. However, these deposits were not analyzed using organic petrology. Deacon (1993) argues that fine charred organic material at KRM may have been waste from edible plants, but other materials such as grass bedding could also have been burnt at the site. It is unclear whether this is deliberate burning as site maintenance (e.g., Wadley et al. 2011, 2020) or if wood fires were made on discarded organic matter.

4.3.5 | Shell

The densely packed roughly horizontal shell in MF 5.1 is consistent with a midden (Aldeias and Bicho 2016; Villagran et al. 2011; Villagran 2019). The occurrence of some in situ fragmentation of the shell and bone suggests some trampling, but much of the compression is by overburden. This resulted in a loss of stratigraphic detail, and some of the sand and ash may have been distinct deposits interbedded with the shell (Wurz et al. 2022, Figure 10b). Secondary calcification was due to the percolation of calcium-enriched dripwater (Wurz et al. 2022).

4.3.6 | Fine Siliceous Sediment

Although siliceous silt and clay are present in low quantities in many deposits, MF 6.1 is the only MF type that is dominated by this sediment. Similar discontinuous stringers of geogenic fine sediment seem to represent periods of surface stability at Die Kelders (Goldberg 2000, 54). In this case, it appears most likely that dripwater enriched in ferrous minerals from iron-rich veins in the quartzite-transported siliceous silt and clay weathered from the landscape surface or the host rock itself down into the cave. The precipitated iron is in the form of goethite, a common secondary mineral in caves formed in a wide range of lithologies (Hill and Forti 1997). This deposit could represent surficial ponding, as suggested by Deacon and Geleijnse (1988) for the upper surface of the SBLS, but the underlying deposits are far sandier here (Figure 8) than the sediments they described, so this appears unlikely. The increasingly sandy nature of the deposit moving across its sampled extent might reflect increasing distance from the drip location or could be the product of localized post-depositional mixing with the overlying sands.

4.4 | Anthropogenic Features

The sampled deposits contain variably preserved anthropogenic features, which include hearths (Figures 13a–e and 14), middens (Figure 7), dumps (Figures 6 and 15), and palimpsests deformed and mixed by trampling (Figure 13c). The distribution of different deposits is presented in Figure 16. Two features indicative of different behaviors are described and discussed below.

Much of slide 304 A is a stacked hearth feature (Figure 14). There is no ash layer above the basal charred MSU, and the overlying sand (MF 1.2) contains reworked ash and small bone fragments. The charred layer appears intact, and its fabric (Figure 14a) is inconsistent with experimental swept hearths (Miller et al. 2010). The ash must have been removed by a natural process gentle enough to cause limited disturbance to the base. Although wind may have removed some ash, it is likely that much of it was dissolved. Another charcoal-rich deposit higher up is also similarly overlain unconformably by ashy sand (Figure 14c). The tissue structures of charcoal fragments in the two charcoal-rich deposits are identical (online Supporting Information), and their reflectance values (Supporting Information S1: Figures S3 and S5) are very similar, suggesting the same wood and burning conditions for both. There is a final unconformity at the top of the stack where ash has been reworked, including in the form of angular aggregates.

Internal lamination in the ash packets (Figure 14b) indicates that, consistent with experimental work (Karkanas 2021), these deposits were formed by repeated fires. The number of firings

15206548, 2025, 2, Downloaded from https://onlinelibrary.wiley.com/doi/10.1002/gea.70005 by University Of Witwatersrand, Wiley Online Library on [22/10/2025]. See the Terms and Conditions (https://onlinelibrary.wiley.com/terms-and-conditions) on Wiley Online Library for rules of use; OA articles are governed by the applicable Creative Commons License

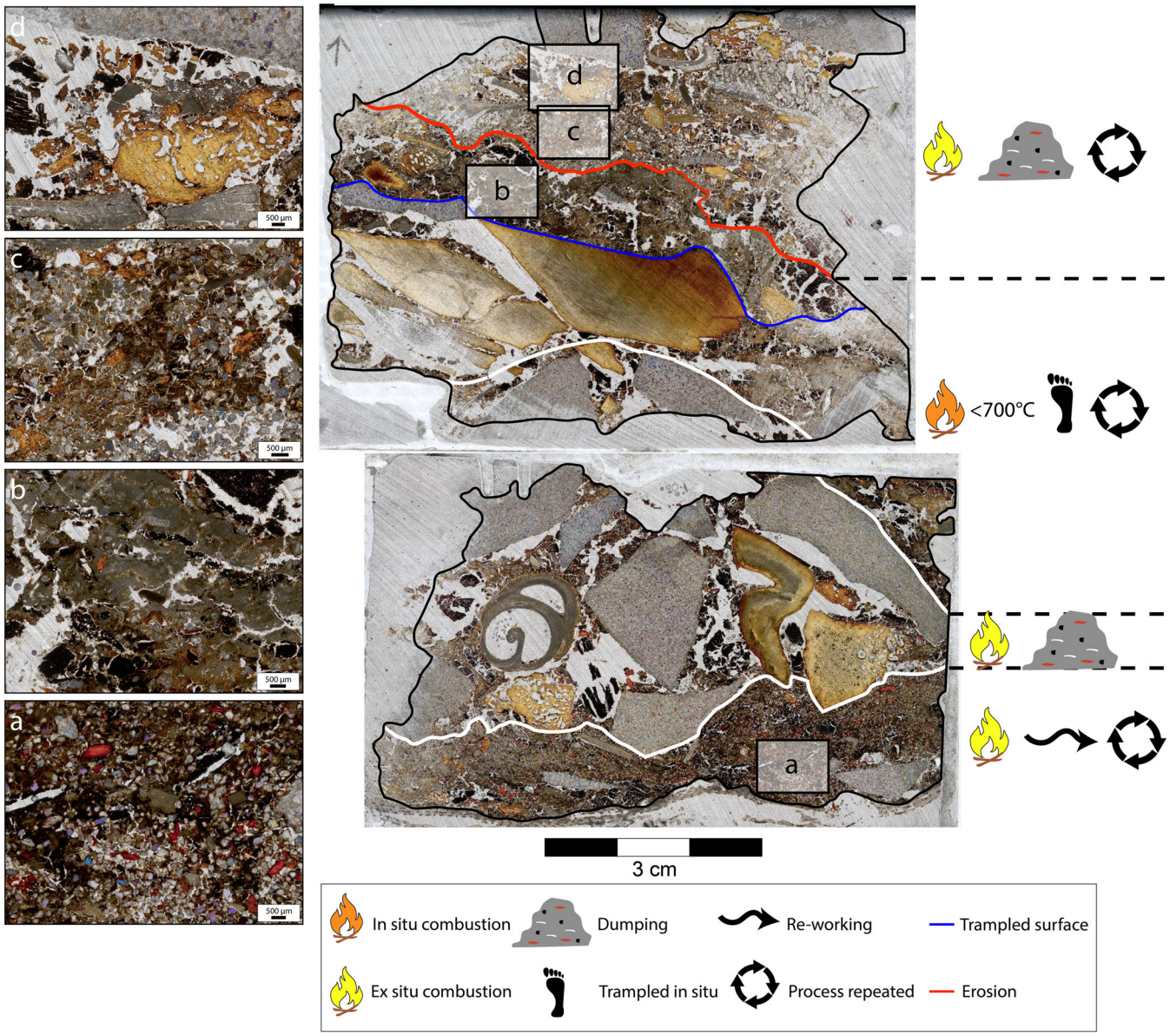


FIGURE 15 | Summary of the anthropogenic processes involved in forming the deposits in slides 301 A (above) and 301B (below), SBLS, western profile. All insets are in PPL and are arranged in a stratigraphic order on the left side of the figure. (a) Ashy sand (MF 1.2), which is particularly rich in the ashy and charred matrix, micro-charcoal, and small (apparently) burnt bone fragments. (b) Lightly trampled ash of MF 3.2. Note the undulating thin charred lenses and the variable recrystallization and phosphatization. (c) Area of the MF 1.3 deposits, which is particularly rich in ashy and charred organic matrix. (d) Portion of the MF 1.3 deposits, which is dominated by sand-sized and larger bone and shell fragments, with some charcoal but little matrix. The broken shell and crushed bone (unburnt in this case) are rare examples of in situ breakage of clasts.

between erosional events suggests a high frequency of use, while the lack of evidence for trampling and hearth maintenance indicates comparatively short occupations and/or small groups of occupants (Karkanas et al. 2015; Haaland et al. 2021). The period of exposure required for erosion/dissolution to take place in different cave contexts is unclear, but this can occur rapidly in open-air settings (Shahack-Gross et al. 2004; Mallol et al. 2007). Unfortunately, the loss of ash makes it difficult to assess how many occupational periods occurred. Although the time ranges for both occupation and abandonment are uncertain, people clearly returned and used the same space for the same purpose across multiple occupations, including after absences in which the hearth was partly buried by a thin layer of sand.

The sequence of events in sample 301 is illustrated in Figure 15. The lowermost deposits (MF 1.2) are notably richer in anthropogenic matrix and sand-sized pieces of charcoal and bone than is normal for this MF (Figure 15a), indicating a relatively high input of hearth materials. The overlying dumped deposits (MFs 1.3 and 2.2) indicate multiple hearth-cleaning events in a period short enough that distinct geogenic deposits did not form between them. The evidence throughout 301 for hearth maintenance activities, the mixed use of space (hearths between dumped deposits), and the light trampling of the hearths and of the upper dumped deposits (Figure 15d) are all suggestive of a period of intensive occupation in which anthropogenic materials accumulated rapidly at this location (Miller et al. 2013; Karkanas et al. 2015).

15206548, 2025, 2, Downloaded from https://onlinelibrary.wiley.com/doi/10.1002/gea.70005 by University Of Witwatersrand, Wiley Online Library on [22/10/2025]. See the Terms and Conditions (https://onlinelibrary.wiley.com/terms-and-conditions) on Wiley Online Library for rules of use; OA articles are governed by the applicable Creative Commons License

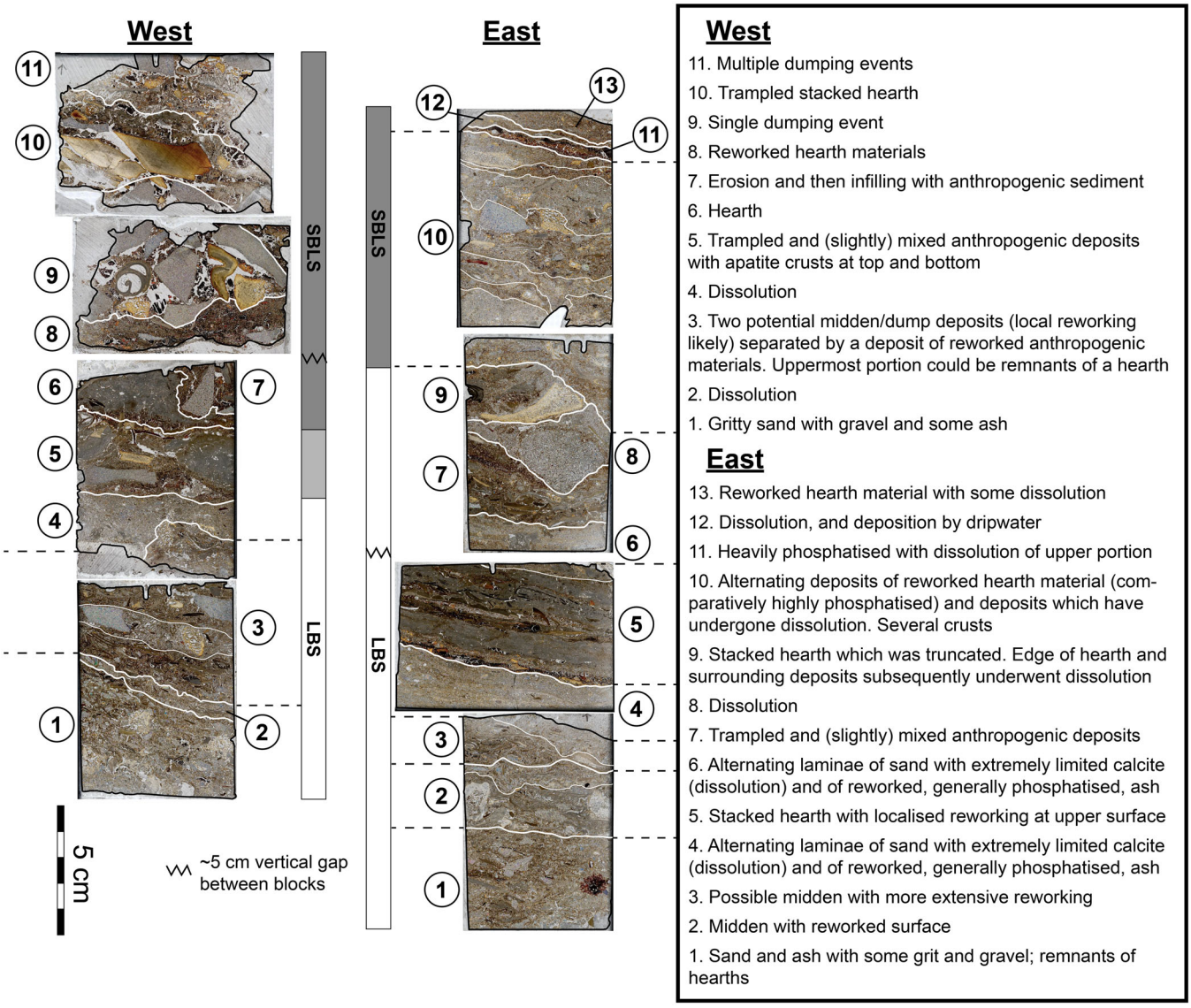


FIGURE 16 | Interpretive microstratigraphy of the western (samples 302 and 301) and eastern (samples 304 and 303) profiles. Note that microstratigraphic units have often been grouped due to representing the same general set of processes or due to cycles of multiple repeated events/processes.

4.5 | Diagenesis and Hiatuses

Intact and reworked crusts are present in several parts of the sequence (Figures 12 and 16). Thin localized and/or reworked apatite crusts occur in the basal gravel at the western location. Thicker and less disturbed, sometimes discontinuous, apatite crusts are present in the deposits at the transition between the LBS and SBLS in the west and at the contact between the LBS and SBLS in the east. A roughly linear zone rich in numerous small sub-angular goethite aggregates with sand inclusions (Figure 12d,e) in the eastern SBLS is the reworked remnants of another crust. It likely formed in a similar manner to MF 6.1, but the dripwater contained limited siliceous silt and clay and was more heavily enriched with iron. All crusts indicate periods of surface stability (Hill and Forti 1997; Karkanas 2017; Haaland et al. 2021; Morrissey et al. 2023), followed by differing degrees of disturbance of these surfaces.

Recrystallization, cementation, and phosphatization of ash all improve preservation (despite the destruction of some original ash morphologies) by reducing the potential for dissolution and physical disturbance (Mentzer 2014; Mallol et al. 2017). Repeated firings are also beneficial for ash preservation (Karkanas 2021).

Organic petrology observations of charcoal-rich deposits in 304A reveal the degradation and diagenesis of both charcoal and fat-derived char and variation in the intensity of these processes between MSUs (online Supporting Information). Similar processes were recorded by Larbey et al. (2019) in the LBS at the southern end of the Witness Baulk. Unlike in past work, there is evidence from both micromorphology (Figure 14e) and organic petrology (Supporting Information S1: Figure S6) for the replacement of wood or charcoal by calcite, but this phenomenon is poorly understood. Although these observations are limited to a single slide, they may explain the rarity and variable preservation of hearth bases in the sampled deposits.

15206548, 2025, 2, Downloaded from https://onlinelibrary.wiley.com/doi/10.1002/gea.70005 by University Of Witwatersrand, Wiley Online Library on [22/10/2025]. See the Terms and Conditions (https://onlinelibrary.wiley.com/terms-and-conditions) on Wiley Online Library for rules of use; OA articles are governed by the applicable Creative Commons License

Calcification of bone through precipitation of secondary calcite occurred in some cases, and a few of these bones have undergone subsequent incomplete dissolution of the secondary calcite (Figure 13b). The dissolution of shells (to varying degrees) is common (see the elemental maps in Figures 5–8). Delamination is visible, and this can be confidently attributed to heating in some cases but in others could be a result of the precipitation of salts (Wurz et al. 2022). The bone and shell have been impacted by trampling in many deposits, particularly in the reworked sandy MF types. Trampling has also contributed to a loss of stratigraphic detail due to compression and mixing (Figure 13c).

The microcontextual evidence shows that both physical and chemical processes have impacted the preservation of the shell and bone, but detailed taphonomic studies of excavated assemblages (e.g., Reynard 2022) will provide greater insight into these impacts and any spatial or temporal patterns in occupational intensity. The dissolution of ash and the shell, observed in many deposits, is the most significant destructive diagenetic process and requires greater consideration here.

The alternation of various ash-rich MSUs and the sand of MF 1.1 suggests that the dissolution of calcite at the sampled locations occurred at, or very near, the surface. The length of time a deposit is exposed is controlled by depositional rates, with slower deposition or a depositional hiatus (with or without erosion) both resulting in longer exposure and greater diagenetic potential. The regularity and nature of anthropogenic deposition can have a marked impact on deposit exposure in cave and rockshelter contexts, as it is generally more rapid (but less continuous) than geogenic deposition (Morrissey et al. 2023). Exposure time is not the only potential factor at play. A lower proportion of ash within a deposit reduces the pH buffering effect of calcite, making the dissolution of any ash and shell that is present more likely (Berna et al. 2004; Sherwood et al. 2004; Miller et al. 2013). A deposit containing less ash would be impacted more heavily by the same period of surface exposure than an ashier deposit. The occurrence and intensity of diagenetic processes may also vary over space and time within a site (Schiegl et al. 1996; Goldberg 2000; Wurz et al. 2022), further complicating the matter.

There is a clear spatial pattern in the diagenesis of the LBS, with fewer partially decalcified deposits in the western profile than in the eastern profile (Figures 5–8 and 16). This is even stronger in the SBLS, with no decalcified deposits in the west, and MF 1.1 making up roughly half of the member in the east. The sands in the western SBLS are particularly high in the ashy and fine organic matrix, with a higher density of small charcoal and bone fragments than most other MF 1.2 deposits. In contrast, MF 1.2 MSUs in the east contain less matrix than those in the LBS, with greater ash phosphatization. The MF 1.1 deposits in the eastern SBLS also appear more completely decalcified than those in the LBS. A poorly preserved hearth is the only anthropogenic feature in the eastern SBLS (Figures 13e and 16).

The general pattern of greater dissolution in the east is probably due to cave morphology. The roof is relatively low on the western side of the Witness Baulk but rises steeply on the eastern side (Singer and Wymer 1982, fig. 3.3). Small ledges and crannies are common, and this area is and would have been, more attractive as a bird roosting area due to the greater availability of suitable surfaces with greater physical distance from non-avian predators. A pattern in the distribution of guano should be present unless there have been changes to the ceiling due to rock fall, speleothem development, or other factors. Periods with higher concentrations of guano in this location probably also reduced the attractiveness of using it as an activity area.

The greater difference between the two sampled locations in the SBLS could have been influenced by the decreasing distance between the accumulating deposits and the lower roof in the west, but other factors seem to be more important. Anthropogenic deposition appears to have been markedly higher in the western SBLS (Figure 15), with resulting protection due to shorter exposure times and greater pH buffering. The sudden increase in microfauna and fish remains in the eastern profile seems to reflect less human occupation of the cave and the congregation of birds in this area. In other areas of the site complex, in particular Cave 2, the localized absence of bone appears to reflect particularly intense diagenesis. However, minerals like leucophosphite also form under conditions conducive to bone dissolution (Karkanas et al. 2000) and, although leucophosphite is present in Cave 2 (Wurz et al. 2022), it was not observed in any of these thin sections. This suggests that the increase in the density of microfauna remains is not due to a significant change in the intensity of diagenesis. Alongside the distinguishable microfauna, the MF 1.1 and 1.2 deposits contain more relatively large bone fragments than their counterparts in the LBS, suggesting a reduction in trampling. A reworked iron-rich crust (Figure 12d,e), a heavily phosphatized hearth (Figure 13e), and the silt and clay deposit assigned to MF 6.1 all support the idea of greater surface exposure, including hiatuses, of the SBLS in the east.

The SBLS deposits on either side of the Witness Baulk appear to represent highly contradictory situations. In the west, well-preserved anthropogenic features/deposits show little indication of significant occupational and/or depositional hiatuses. In the east, anthropogenic features are poorly preserved and far less common, with clear evidence of a comparatively low rate of anthropogenic deposition, periods of abandonment, and depositional hiatuses (Figure 16). The proposed explanation is that there were periods of intensive activity in the cave but also periods of abandonment or far lower-intensity occupation. Spatial patterns in both human activities and biogenically driven diagenesis then resulted in greater susceptibility to dissolution and phosphatization in the East and lower potential for these processes in the West. A broadly similar pattern of preservation being controlled by both human choice of where to carry out different activities and geomorphic controls on biological activity (bioturbation in this case) has been inferred at Üçağızlı II Cave in Turkey (Baykara et al. 2015).

This extreme variation in properties highlights the significance of anthropogenic deposition in Cave 1, as spatial and temporal patterns impact the likelihood of distinguishable anthropogenic features and deposits being preserved and studied. Anthropogenic deposits are common in the SBLS at the southern end of the Witness Baulk (Figure 4) and are relatively well preserved, with some hearths surviving significant plastic deformation while remaining otherwise intact (Wurz et al. 2022). As in the

15206548, 2025, 2, Downloaded from https://onlinelibrary.wiley.com/doi/10.1002/gea.70005 by University Of Witwatersrand, Wiley Online Library on [22/10/2025]. See the Terms and Conditions (https://onlinelibrary.wiley.com/terms-and-conditions) on Wiley Online Library for rules of use; OA articles are governed by the applicable Creative Commons License

western location, the high density of anthropogenic deposits and a lower roof likely played a role in this preservation.

5 | Discussion

5.1 | Stratigraphic Implications

Stratigraphic correlation within and between different recesses at KRM is complicated due to both variations and similarities in sedimentary properties and comparatively limited recording during the initial excavations (Morrissey et al. 2022). The new insights into site formation from this study have several significant implications for the stratigraphy of Cave 1 and beyond.

The properties of the SBLS deposits differ significantly between the two sampling locations (Figure 4). If these sets of deposits were encountered on either side of one of Wymer's excavation trenches, without the means to directly track stratigraphic relationships between them, they might easily be considered distinct lithostratigraphic members. Therefore, the specific set of site formation processes, which occurred at a particular location—including a range of potential human behaviors—significantly impacts whether deposits will be correctly correlated (or not correlated) across the site complex.

Plastic deformation of deposits at the western and eastern sample locations is limited in comparison to most of the current excavation area, especially in the east (Figure 4). The limited extent of this contorted bedding across Cave 1 is highlighted by Singer and Wymer (1982, fig. 3.24). This suggests that the deformation is due to the collapse of the large speleothem column (and perhaps other previously excavated pieces) into the deposits, with subsequent uneven loading as overlying deposits accumulated. Although they have been presented as a defining characteristic of the SBLS (e.g., Deacon and Geleijnse 1988), these contortions, and occasional relatively clast-rich zones, which led to the deposits being called the RBS, are not truly representative of this member (Morrissey et al. 2022, 19–20). However, they do represent important localized depositional and/or post-depositional events, which are vital for understanding the deposits in these locations.

Attempts to correlate the MSA I deposits across the site complex have met with mixed success (Morrissey et al. 2022). General similarities in sedimentary properties and stratigraphic position mean that the correlation of the LBS deposits in Cave 1 and Cave 1 A has been uncontroversial. In contrast, suggested correlations of the SBLS with deposits in Cave 1 A (units SCB2 to SCB1) and Cave 1B (Wymer's Layer 10) (Deacon and Geleijnse 1988; Grine et al. 2017) have subsequently been shown to be inaccurate (Morrissey et al. 2022, 2023).

As the SBLS appears to be the product of particularly intensive occupation and a specific set of post-depositional conditions, contemporaneous deposits in these areas would very likely have differing properties. Therefore, it is possible, but not guaranteed, that some of the upper LBS deposits in Cave 1 A could correlate with the SBLS (Morrissey et al. 2022, Figure 9d). The formation of the RS Member in Cave 1B likely spans part of the same period as the LBS in Cave 1 and all or part of the period in which the SBLS was deposited (Morrissey et al. 2023). Any temporal patterning in the composition of MSA I faunal and lithic assemblages excavated at high resolution during the Deacon and Wurz excavations could help with making finer stratigraphic correlations across the site complex independent of lithology (Discamps et al. 2023).

5.2 | Behavioral Significance

The MSA and Middle Palaeolithic are characterized by increasing structuring and maintenance of sites, which, along with many other lines of evidence, provides insight into the evolution of modern human behavior during this period (e.g., McBrearty and Brooks 2000; Conard 2015; Clark et al. 2022; Scerri and Will 2023). Intensity and frequency of occupation and the activities for which a space is used all impact the expenditure of effort and time on structuring and maintenance (Miller et al. 2013; Haaland et al. 2021; Clark et al. 2022).

The MSA I shell middens at KRM are among the few known occurrences pre-dating 100 ka, all at coastal sites in South Africa (Jacobs 2010; Karkanas and Goldberg 2010; Niespolo et al. 2021; Tribolo et al. 2022; Wurz et al. 2022). These features are significant because they show occupational intensity and exploitation of marine resources that were both high enough to result in the formation of distinct shell-dominated dumps (e.g., Deacon 1995; Marean 2014; Niespolo et al. 2021; Wurz et al. 2022). Dumps other than shell middens have received comparatively limited attention in the MSA due to the strong interest in coastal adaptations but still indicate structuring and maintenance of space (Goldberg et al. 2009; Miller et al. 2013).

The intensity of occupation in Cave 1 in the LBS and SBLS appears to have been higher than has been inferred for the MSA I-bearing RS Member in Cave 1B (Morrissey et al. 2023). However, this is somewhat deceptive. Cave 1 is far more sheltered than Cave 1B because it is more closed but also because the mouth of the cave is southeast-facing. In contrast, Cave 1B is particularly exposed to the winter westerlies, which were the most geomorphologically effective winds along the southern Cape coast throughout the Middle and Late Pleistocene (Roberts et al. 2014). Unlike the studied Cave 1 deposit, geogenic units are fairly common in the RS, and anthropogenic deposits are rare and generally poorly preserved (Morrissey et al. 2023). It is almost certain that the rate of geogenic deposition was far higher in Cave 1B. Within the enclosed space of Cave 1, the limited geogenic sediment would have been easily mixed with anthropogenic sediment by trampling and site maintenance activities even without very regular or intensive occupation. The anthropogenic signal in Cave 1B would be comparatively diluted due to the more rapid geogenic deposition, even without the difference in the preservation potential of ash and any possible variation in how the two spaces were utilized.

The anthropogenic features/deposits in the sampled LBS do not seem to indicate a stable level of occupational intensity throughout the formation of the member. The properties of the SBLS have long been suggested to represent significant anthropogenic input, with Singer and Wymer (1982, 16) referring to these deposits as “occupational soil”. Given the excellent preservation of some features in the LBS in Cave 1 (Larbey et al. 2019; Wurz et al. 2022; this study) and the nature of the deposits in the SBLS at the western sample location (Figure 15), the significant

15206548, 2025, 2, Downloaded from https://onlinelibrary.wiley.com/doi/10.1002/gea.70005 by University Of Witwatersrand, Wiley Online Library on [22/10/2025]. See the Terms and Conditions (https://onlinelibrary.wiley.com/terms-and-conditions) on Wiley Online Library for rules of use; OA articles are governed by the applicable Creative Commons License

increase in anthropogenic sedimentary components in the SBLS must reflect a change in occupational intensity and/or reduced geogenic deposition rather than widely differing preservation potentials. A period of sea-level regression and the resulting hypothesized formation of a barrier dune between KRM and the sea (Deacon and Geleijnse 1988; Deacon 1995) would have led to reduced aeolian deposition across the site complex. This possibility is supported by evidence for a notable reduction in allogenic deposition in Cave 1B associated with the end of the MSA I (Morrissey et al. 2023).

Changes in occupational intensity over time, with differing degrees and types of site structuring and maintenance and other anthropogenic disturbances, have been noted at several South African MSA sites studied at the microscale (Goldberg et al. 2009; Wadley et al. 2011; Miller et al. 2013; Karkanas et al. 2015; Haaland et al. 2021). At Blombos Cave and Pinnacle Point 5-6, these changes in site use correspond to the transition from MIS 5 to the colder MIS 4 and likely reflect a range of adaptations to changing resource availability (some driven by lower sea levels) and physical conditions (Karkanas et al. 2015; Haaland et al. 2021).

The MSA I deposits formed during a period that includes MIS 5e and early MIS 5 d, before 110 ka. This period is associated with the early stages of regression from the sea-level highstand/s, which occurred during MIS 5e (Cooper and Green 2021). Changes in local resource availability, the attractiveness of KRM for occupation, and aeolian depositional rates would have occurred, but it is not currently possible to confidently link the boundary between the LBS and SBLS to any particular stage (and associated sea-level estimate) in this period without a secure date for this boundary.

The ongoing excavation and analysis of MSA I lithic and faunal assemblages, along with anthropogenic features in the Witness Baulk, will provide more detailed and better-contextualized evidence to further assess changes in occupational intensity (e.g., Haaland et al. 2021). These data, along with any further dating of the MSA I deposits, could also provide clarity on what role (if any) sea level and other environmental or geomorphic factors played in driving behaviors that led to changing occupational intensities within and between members and/or causing changes in the rate of geogenic deposition in Cave 1.

6 | Conclusions

The application of a microscale geoarchaeological approach to deposits north of the Witness Baulk excavation has provided insight into events that took place in periods of hours or days and revealed the cumulative effects of thousands of years of depositional and diagenetic patterns. The results have improved our understanding of the MSA I deposits in this part of Cave 1 and, along with previous work on the southern end of the baulk, provide vital context to the interpretation of excavated assemblages and features.

The significant roles of both natural processes and human behavior in forming deposits, and clear evidence for spatial patterns in both, highlight the importance of clarifying site formation processes when attempting to understand stratigraphic relationships over even comparatively short distances. As the lithostratigraphic members and sub-members have often been presented as monolithic, and human behavior is typically interpreted in large time slices spanning entire cultural phases, this also has important implications for how excavated assemblages are viewed.

Given that the MSA I pre-dates 110 ka, evidence for the structuring and maintenance of space within Cave 1 throughout this period is significant. The behavioral insights gained from individual anthropogenic features/deposits are highly informative about specific events or sequences of related events, but the patterns of both intra- and inter-member variation in occupational intensity and/or frequency provide a broader view of changes in the use of the site over time, although potential variation in geogenic depositional rates is a complicating factor. Integration with data from excavated assemblages and a better understanding of the ages of the LBS and SBLS will provide a fuller picture of these changes and the context with which to better understand human adaptation to varying local and regional conditions during a period of significant global change.

Author Contributions

Peter Morrissey: conceptualization, funding acquisition, investigation, visualization, writing – original draft preparation. **Sarah Wurz:** conceptualization, funding acquisition, writing – review and editing. **Bertrand Ligouis:** investigation, writing – review and editing. **Susan Mentzer:** conceptualization, funding acquisition, investigation, writing – review and editing.

Acknowledgments

Kathryn Croll assisted with micromorphology sampling and took field photographs. Thin sections were prepared by Panos Kritikakis. The support of GENUS: DSI-NRF Centre of Excellence in Palaeosciences (UID 86073) toward this research in the form of grants to Peter Morrissey and Sarah Wurz is hereby acknowledged. The authors also acknowledge the Palaeontological Scientific Trust (PAST) for a fieldwork grant to Sarah Wurz and a doctoral support grant to Peter Morrissey, as well as the Baden-Württemberg Ministerium für Wissenschaft, Forschung und Kunst for funding a research fellowship to Peter Morrissey to facilitate microscale analysis. Opinions expressed and conclusions arrived at are those of the authors and are not necessarily to be attributed to any of these funders. Two anonymous reviewers and Sarah Sherwood provided comments that led to the improvement of this manuscript.

Conflicts of Interest

The authors delare no conflicts of interest.

Data Availability Statement

Most of the data that supports the findings of this study are available in the supporting material of this article. Any remaining data are available from the corresponding author upon reasonable request.

Endnotes

[1]Note that, despite the use of the term "soils", the SBLS and other deposits within Cave 1 whose names include the term are not pedogenic in origin. The term has frequently been used synonymously with "sediment" at KRM since the earliest research at the site (see further discussion in Morrissey et al. 2022, 2023).

References

Aldeias, V., and N. Bicho. 2016. "Embedded Behavior: Human Activities and the Construction of the Mesolithic Shellmound of Cabeço da

15206548, 2025, 2, Downloaded from https://onlinelibrary.wiley.com/doi/10.1002/gea.70005 by University Of Witwatersrand, Wiley Online Library on [22/10/2025]. See the Terms and Conditions (https://onlinelibrary.wiley.com/terms-and-conditions) on Wiley Online Library for rules of use; OA articles are governed by the applicable Creative Commons License

Amoreira, Muge, Portugal." *Geoarchaeology* 31: 530–549. https://doi.org/10.1002/geo.21573.

Aldeias, V., S. Gur-Arieh, R. Maria, P. Monteiro, and P. Cura. 2019. "Shell We Cook It? An Experimental Approach to the Micro-archaeological Record of Shellfish Roasting." *Archaeological and Anthropological Sciences* 11: 389–407. https://doi.org/10.1007/s12520-016-0413-1.

Baykara, İ., S. M. Mentzer, M. C. Stiner, Y. Asmerom, E. S. Güleç, and S. L. Kuhn. 2015. "The Middle Paleolithic Occupations of Üçağızlı II Cave (Hatay, Turkey): Geoarcheological and Archeological Perspectives." *Journal of Archaeological Science: Reports* 4: 409–426. https://doi.org/10.1016/j.jasrep.2015.09.022.

Berna, F. 2017. "FTIR Microscopy." In *Archaeological Soil and Sediment Micromorphology*, edited by C. Nicosia and G. Stoops, 411–415. Wiley Blackwell.

Berna, F., A. Matthews, and S. Weiner. 2004. "Solubilities of Bone Mineral From Archaeological Sites: The Recrystallization Window." *Journal of Archaeological Science* 31: 867–882. https://doi.org/10.1016/j.jas.2003.12.003.

Borrego, A. G., C. V. Araujo, A. Balke, et al. 2006. "Influence of Particle and Surface Quality on the Vitrinite Reflectance of Dispersed Organic Matter: Comparative Exercise Using Data From the Qualifying System for Reflectance Analysis Working Group of ICCP." *International Journal of Coal Geology* 68: 151–170. https://doi.org/10.1016/j.coal.2006.02.002.

Butzer, K. W. 1982. "Geomorphology and Sediment Stratigraphy." In *The Middle Stone Age at Klasies River Mouth in South Africa*, edited by R. Singer and J. Wymer, 33–42. Chicago University Press.

Canti, M. G., and J. E. Brochier. 2017. "Plant ash." In *Archaeological Soil and Sediment Micromorphology*, edited by C. Nicosia and G. Stoops, 147–154. Wiley Blackwell.

Clark, A. E., S. Ranlett, and M. C. Stiner. 2022. "Domestic Spaces as Crucibles of Paleolithic Culture: An Archaeological Perspective." *Journal of Human Evolution* 172: 103266. https://doi.org/10.1016/j.jhevol.2022.103266.

Clark, J. L., and B. Ligouis. 2010. "Burned Bone in the Howieson's Poort and Post-Howieson's Poort Middle Stone Age Deposits at Sibudu (South Africa): Behavioral and Taphonomic Implications." *Journal of Archaeological Science* 37: 2650–2661. https://doi.org/10.1016/j.jas.2010.06.001.

Conard, N. J. 2015. "Cultural Evolution During the Middle and Late Pleistocene in Africa and Eurasia." In *Handbook of Paleoanthropology*, edited by W. Henke and I. Tattersall, 2465–2508. Springer.

Cooper, J. A. G., and A. N. Green. 2021. "A Standardized Database of Marine Isotope Stage 5e Sea-Level Proxies in Southern Africa (Angola, Namibia and South Africa)." *Earth System Science Data* 13: 953–968. https://doi.org/10.5194/essd-13-953-2021.

Courty, M. A. 2001. "Microfacies Analysis Assisting Archaeological Stratigraphy." In *Earth Sciences and Archaeology*, edited by P. Goldberg, V. T. Holliday, and C. F. Ferring, 205–239. Springer.

Deacon, H. J. 1989. "Late Pleistocene Palaeoecology and Archaeology in the Southern Cape, South Africa." In *The Human Revolution*, edited by P. Mellars and C. B. Stringer, 547–564. Edinburgh University Press.

Deacon, H. J. 1993. "Planting an Idea: An Archaeology of Stone Age Gatherers in South Africa." *South African Archaeological Bulletin* 48: 86–93.

Deacon, H. J. 1995. "Two Late Pleistocene-Holocene Archaeological Depositories From the Southern Cape, South Africa." *South African Archaeological Bulletin* 50: 121–131.

Deacon, H. J. 2008. "The Context of the 1967–8 Sample of Human Remains From Cave 1 Klasies River Main Site." *South African Archaeological Society Goodwin Series* 10: 143–149.

Deacon, H. J., and V. B. Geleijnse. 1988. "The Stratigraphy and Sedimentology of the Main Site Sequence, Klasies River, South Africa." *South African Archaeological Bulletin* 43: 5–14.

Discamps, E., M. Thomas, C. Dancette, et al. 2023. "Breaking Free From Field Layers: The Interest of Post-Excavation Stratigraphies (PES) for Producing Reliable Archaeological Interpretations and Increasing Chronological Resolution." *Journal of Paleolithic Archaeology* 6: 29. https://doi.org/10.1007/s41982-023-00155-x.

Feathers, J. K. 2002. "Luminescence Dating in Less Than Ideal Conditions: Case Studies From Klasies River Main Site and Duinefontein, South Africa." *Journal of Archaeological Science* 29: 177–194. https://doi.org/10.1006/jasc.2001.0685.

Goldberg, P. 2000. "Micromorphology and Site Formation at Die Kelders Cave I, South Africa." *Journal of Human Evolution* 38: 43–90. https://doi.org/10.1006/jhev.1999.0350.

Goldberg, P. 2003. "Some observations on Middle and Upper Palaeolithic Ashy Cave and Rockshelter deposits in the Near East." In *More Than Meets the Eye: Studies on Upper Palaeolithic Diversity in the Near East*, edited by A. N. Goring-Morris and A. Belfer-Cohen, 19–32. Oxbow Books.

Goldberg, P., C. E. Miller, S. Schiegl, et al. 2009. "Bedding, Hearths, and Site Maintenance in the Middle Stone Age of Sibudu Cave, Kwazulu-Natal, South Africa." *Archaeological and Anthropological Sciences* 1: 95–122. https://doi.org/10.1007/s12520-009-0008-1.

Grine, F. E., S. Wurz, and C. W. Marean. 2017. "The Middle Stone Age Human Fossil Record From Klasies River Main Site." *Journal of Human Evolution* 103: 53–78. https://doi.org/10.1016/j.jhevol.2016.12.001.

Haaland, M. M., D. E. Friesem, C. E. Miller, and C. S. Henshilwood. 2017. "Heat-Induced Alteration of Glauconitic Minerals in the Middle Stone Age Levels of Blombos Cave, South Africa: Implications for Evaluating Site Structure and Burning Events." *Journal of Archaeological Science* 86: 81–100. https://doi.org/10.1016/j.jas.2017.06.008.

Haaland, M. M., C. E. Miller, O. F. Unhammer, et al. 2021. "Geoarchaeological Investigation of Occupation Deposits in Blombos Cave in South Africa Indicate Changes in Site Use and Settlement Dynamics in the Southern Cape During MIS 5b–4." *Quaternary Research* 100: 170–223. https://doi.org/10.1017/qua.2020.75.

Henderson, Z. 1992. "The Context of Some Middle Stone Age Hearths at Klasies River Shelter 1b: Implications for Understanding Human Behaviour." *Southern African Field Archaeology* 1: 14–26.

Hill, C., and P. Forti. 1997. *Cave Minerals of the World*, 2nd ed. National Speleological Society.

Jacobs, Z. 2010. "An OSL Chronology for the Sedimentary Deposits From Pinnacle Point Cave 13B—A Punctuated Presence." *Journal of Human Evolution* 59: 289–305. https://doi.org/10.1016/j.jhevol.2010.07.010.

Karkanas, P. 2017. "Guano." In *Archaeological Soil and Sediment Micromorphology*, edited by C. Nicosia and G. Stoops, 83–90. Wiley Blackwell.

Karkanas, P. 2021. "All about Wood Ash: Long Term Fire Experiments Reveal Unknown Aspects of the Formation and Preservation of Ash With Critical Implications on the Emergence and Use of Fire in the Past." *Journal of Archaeological Science* 135: 105476. https://doi.org/10.1016/j.jas.2021.105476.

Karkanas, P., O. Bar-Yosef, P. Goldberg, and S. Weiner. 2000. "Diagenesis in Prehistoric Caves: The Use of Minerals That Form In Situ to Assess the Completeness of the Archaeological Record." *Journal of Archaeological Science* 27: 915–929. https://doi.org/10.1006/jasc.1999.0506.

Karkanas, P., K. S. Brown, E. C. Fisher, Z. Jacobs, and C. W. Marean. 2015. "Interpreting Human Behavior From Depositional Rates and Combustion Features Through the Study of Sedimentary Microfacies at Site Pinnacle Point 5–6, South Africa." *Journal of Human Evolution* 85: 1–21. https://doi.org/10.1016/j.jhevol.2015.04.006.

15206548, 2025, 2, Downloaded from https://onlinelibrary.wiley.com/doi/10.1002/gea.70005 by University Of Witwatersrand, Wiley Online Library on [22/10/2025]. See the Terms and Conditions (https://onlinelibrary.wiley.com/terms-and-conditions) on Wiley Online Library for rules of use; OA articles are governed by the applicable Creative Commons License

Karkanas, P., and P. Goldberg. 2010. "Site Formation Processes at Pinnacle Point Cave 13B (Mossel Bay, Western Cape Province, South Africa): Resolving Stratigraphic and Depositional Complexities With Micromorphology." *Journal of Human Evolution* 59: 256–273. https://doi.org/10.1016/j.jhevol.2010.07.001.

Karkanas, P., C. Marean, M. Bar-Matthews, Z. Jacobs, E. Fisher, and K. Braun. 2021. "Cave Life Histories of Non-Anthropogenic Sediments Help us Understand Associated Archaeological Contexts." *Quaternary Research* 99: 270–289. https://doi.org/10.1017/qua.2020.72.

Karkanas, P., R. Shahack-Gross, A. Ayalon, et al. 2007. "Evidence for Habitual Use of Fire at the End of the Lower Paleolithic: Site Formation Processes at Qesem Cave, Israel." *Journal of Human Evolution* 53: 197–212. https://doi.org/10.1016/j.jhevol.2007.04.002.

Larbey, C., S. M. Mentzer, B. Ligouis, S. Wurz, and M. K. Jones. 2019. "Cooked Starchy Food in Hearths Ca. 120 kya and 65 kya (MIS 5e and MIS 4) From Klasies River Cave, South Africa." *Journal of Human Evolution* 131: 210–227. https://doi.org/10.1016/j.jhevol.2019.03.015.

Ligouis, B. 2017. "Reflected Light." In *Archaeological Soil and Sediment Micromorphology*, edited by C. Nicosia and G. Stoops, 461–470. Wiley Blackwell.

Mallol, C., C. M. Hernández, D. Cabanes, et al. 2013. "The Black Layer of Middle Palaeolithic Combustion Structures. Interpretation and Archaeostratigraphic Implications." *Journal of Archaeological Science* 40: 2515–2537. https://doi.org/10.1016/j.jas.2012.09.017.

Mallol, C., F. W. Marlowe, B. M. Wood, and C. C. Porter. 2007. "Earth, Wind, and Fire: Ethnoarchaeological Signals of Hadza Fires." *Journal of Archaeological Science* 34: 2035–2052. https://doi.org/10.1016/j.jas.2007.02.002.

Mallol, C., S. M. Mentzer, and C. E. Miller. 2017. "Combustion Features." In *Archaeological Soil and Sediment Micromorphology*, edited by C. Nicosia and G. Stoops, 299–330. Wiley Blackwell.

Marcazzan, D., C. E. Miller, and N. J. Conard. 2022. "Burning, Dumping, and Site Use During the Middle and Upper Palaeolithic at Hohle Fels Cave, SW Germany." *Archaeological and Anthropological Sciences* 14: 178. https://doi.org/10.1007/s12520-022-01647-7.

Marean, C. W. 2014. "The Origins and Significance of Coastal Resource Use in Africa and Western Eurasia." *Journal of Human Evolution* 77: 17–40. https://doi.org/10.1016/j.jhevol.2014.02.025.

McBrearty, S., and A. S. Brooks. 2000. "The Revolution That Wasn't: A New Interpretation of the Origin of Modern Human Behavior." *Journal of Human Evolution* 39: 453–563. https://doi.org/10.1006/jhev.2000.0435.

Mentzer, S. M. 2011. "*Macro- and Micro-Scale Geoarchaeology of Üçağızlı Caves I and II, Hatay, Turkey*." Unpublished doctoral dissertation, University of Arizona.

Mentzer, S. M. 2014. "Microarchaeological Approaches to the Identification and Interpretation of Combustion Features in Prehistoric Archaeological Sites." *Journal of Archaeological Method and Theory* 21: 616–668. https://doi.org/10.1007/s10816-012-9163-2.

Mentzer, S. M. 2017. "Micro XRF." In *Archaeological Soil and Sediment Micromorphology*, edited by C. Nicosia and G. Stoops, 431–440. Wiley Blackwell.

Miller, C. E., N. J. Conard, P. Goldberg, and F. Berna. 2010. "Dumping, Sweeping and Trampling: Experimental Micromorphological Analysis of Anthropogenically Modified Combustion Features." *Palethnologie* 2: 25–37. https://doi.org/10.4000/palethnologie.8197.

Miller, C. E., P. Goldberg, and F. Berna. 2013. "Geoarchaeological Investigations at Diepkloof Rock Shelter, Western Cape, South Africa." *Journal of Archaeological Science* 40: 3432–3452. https://doi.org/10.1016/j.jas.2013.02.014.

Miller, C. E., S. M. Mentzer, C. Berthold, et al. 2016. "Site-Formation Processes at Elands Bay Cave, South Africa." *Southern African Humanities* 29: 69–128.

Morrissey, P., S. M. Mentzer, and S. Wurz. 2022. "A Critical Review of the Stratigraphic Context of the MSA I and II at Klasies River Main Site, South Africa." *Journal of Paleolithic Archaeology* 5: 5. https://doi.org/10.1007/s41982-022-00110-2.

Morrissey, P., S. M. Mentzer, and S. Wurz. 2023. "The Stratigraphy and Formation of Middle Stone Age Deposits in Cave 1B, Klasies River Main Site, South Africa, With Implications for the Context, Age, and Cultural Association of the KRM 41815/SAM-AP 6222 Human Mandible." *Journal of Human Evolution* 183: 103414. https://doi.org/10.1016/j.jhevol.2023.103414.

Niespolo, E. M., W. D. Sharp, G. Avery, and T. E. Dawson. 2021. "Early, Intensive Marine Resource Exploitation by Middle Stone Age Humans at Ysterfontein 1 Rockshelter, South Africa." *Proceedings of the National Academy of Sciences of the United States of America* 118: e2020042118. https://doi.org/10.1073/pnas.2020042118.

Rentzel, P., C. Nicosia, A. Gebhardt, D. Bronnimann, C. Pümpin, and K. Ismail-Meyer. 2017. "Trampling, Poaching and the Effect of Traffic." In *Archaeological Soil and Sediment Micromorphology*, edited by C. Nicosia and G. Stoops, 281–297. Wiley Blackwell.

Reynard, J. P. 2022. "Human Occupational Intensity and Palaeoecology at Klasies River From MIS 5-3: Preliminary Taphonomic Analyses of Faunal Remains From the Deacon and Wurz Excavations." *Frontiers in Earth Science* 10: 9745821. https://doi.org/10.3389/feart.2022.974582.

Roberts, D., H. Cawthra, and C. Musekiwa. 2014. "Dynamics of Late Cenozoic Aeolian Deposition Along the South African Coast: A Record of Evolving Climate and Ecosystems." *Geological Society, London, Special Publications* 388: 353–387. https://doi.org/10.1144/SP388.11.

Scerri, E. M. L., and M. Will. 2023. "The Revolution That Still Isn't: The Origins of Behavioral Complexity in *Homo sapiens*." *Journal of Human Evolution* 179: 103358. https://doi.org/10.1016/j.jhevol.2023.103358.

Schiegl, S., P. Goldberg, O. Bar-Yosef, and S. Weiner. 1996. "Ash Deposits in Hayonim and Kebara Caves, Israel: Macroscopic, Microscopic and Mineralogical Observations, and Their Archaeological Implications." *Journal of Archaeological Science* 23: 763–781. https://doi.org/10.1006/jasc.1996.0071.

Schiegl, S., P. Goldberg, H.-U. Pfretzschner, and N. J. Conard. 2003. "Paleolithic Burnt Bone Horizons From the Swabian Jura: Distinguishing Between In Situ Fireplaces and Dumping Areas." *Geoarchaeology* 18: 541–565. https://doi.org/10.1002/gea.10080.

Shahack-Gross, R., F. Marshall, K. Ryan, and S. Weiner. 2004. "Reconstruction of Spatial Organization in Abandoned Maasai Settlements: Implications for Site Structure in the Pastoral Neolithic of East Africa." *Journal of Archaeological Science* 31: 1395–1411. https://doi.org/10.1016/j.jas.2004.03.003.

Sherwood, S. C., B. N. Driskell, A. R. Randall, and S. C. Meeks. 2004. "Chronology and Stratigraphy at Dust Cave, Alabama." *American Antiquity* 69: 533–554. https://doi.org/10.2307/4128405.

Simões, C. D., and V. Aldeias. 2022. "Thermo-Microstratigraphy of Shells Reveals Invisible Fire Use and Possible Cooking in the Archaeological Record." *Frontiers in Earth Science* 10: 869487. https://doi.org/10.3389/feart.2022.869487.

Singer, R., and J. Wymer. 1982. *The Middle Stone Age at Klasies River Mouth in South Africa*. Chicago University Press.

Stepka, Z., I. Azuri, L. K. Horwitz, M. Chazan, and F. Natalio. 2022. "Hidden Signatures of Early Fire at Evron Quarry (1.0 to 0.8 Mya)." *Proceedings of the National Academy of Sciences* 119: e2123439119. https://doi.org/10.1073/pnas.2123439119.

Stoops, G. 2021. *Guidelines for Analysis and Description of Soil and Regolith Thin Sections*, 2nd ed. Wiley.

Sýkorová, I., W. Pickel, K. Christanis, M. Wolf, G. H. Taylor, and D. Flores. 2005. "Classification of Huminite—ICCP System 1994." *International Journal of Coal Geology* 62: 85–106. https://doi.org/10.1016/j.coal.2004.06.006.

15206548, 2025, 2, Downloaded from https://onlinelibrary.wiley.com/doi/10.1002/gea.70005 by University Of Witwatersrand, Wiley Online Library on [22/10/2025]. See the Terms and Conditions (https://onlinelibrary.wiley.com/terms-and-conditions) on Wiley Online Library for rules of use; OA articles are governed by the applicable Creative Commons License

Taylor, G. H., M. Teichmüller, A. Davis, C. F. K. Diessel, R. Littke, and P. Robert. 1998. *Organic Petrology*. Gehrüder Borntraeger.

Thackeray, A. I. 1992. "The Middle Stone Age South of the Limpopo River." *Journal of World Prehistory* 6: 385–440.

Thompson, T. J. U., M. Islam, and M. Bonniere. 2013. "A New Statistical Approach for Determining the Crystallinity of Heat-Altered Bone Mineral From FTIR Spectra." *Journal of Archaeological Science* 40: 416–422. https://doi.org/10.1016/j.jas.2012.07.008.

Toffolo, M. B. 2021. "The Significance of Aragonite in the Interpretation of the Microscopic Archaeological Record." *Geoarchaeology* 36: 149–169. https://doi.org/10.1002/gea.21816.

Tribolo, C., N. Mercier, L. Martin, et al. 2022. "Luminescence Dating Estimates for the Coastal MSA Sequence of Hoedjiespunt 1 (South Africa)." *Journal of Archaeological Science: Reports* 41: 103320. https://doi.org/10.1016/j.jasrep.2021.103320.

Villagran, X. S. 2014. "Experimental Micromorphology on Burnt Shells of *Anomalocardia brasiliana* (Gmelin 1791) (Bivalvia, Veneridae) and Its Potential for Identification of Combustion Features on Shell-Matrix Sites." *Geoarchaeology* 29: 389–396. https://doi.org/10.1002/gea.21486.

Villagran, X. S. 2019. "The Shell Midden Conundrum: Comparative Micromorphology of Shell-Matrix Sites From South America." *Journal of Archaeological Method and Theory* 26: 344–395. https://doi.org/10.1007/s10816-018-9374-2.

Villagran, X. S., A. L. Balbo, M. Madella, A. Vila, and J. Estevez. 2011. "Stratigraphic and Spatial Variability in Shell Middens: Microfacies Identification at the Ethnohistoric Site Tunel VII (Tierra del Fuego, Argentina)." *Archaeological and Anthropological Sciences* 3: 357–378. https://doi.org/10.1007/s12520-011-0074-z.

Wadley, L. 2015. "Those Marvellous Millennia: The Middle Stone Age of Southern Africa." *Azania: Archaeological Research in Africa* 50: 155–226. https://doi.org/10.1080/0067270X.2015.1039236.

Wadley, L., I. Esteban, P. de la Peña, et al. 2020. "Fire and Grass-Bedding Construction 200 Thousand Years Ago at Border Cave, South Africa." *Science* 369: 863–866. https://doi.org/10.1126/science.abc7239.

Wadley, L., C. Sievers, M. Bamford, P. Goldberg, F. Berna, and C. Miller. 2011. "Middle Stone Age Bedding Construction and Settlement Patterns at Sibudu, South Africa." *Science* 334: 1388–1391. https://doi.org/10.1126/science.1213317.

Wurz, S. 2002. "Variability in the Middle Stone Age Lithic Sequence, 115,000–60,000 Years Ago at Klasies River, South Africa." *Journal of Archaeological Science* 29: 1001–1015. https://doi.org/10.1006/jasc.2001.0799.

Wurz, S. 2023. "Klasies River Main Site, South Africa." In *Handbook of Pleistocene Archaeology of Africa: Hominin Behavior, Geography, and Chronology*, edited by A. Beyin, D. K. Wright, J. Wilkins, and D. I. Olszewski, 1531–1547. Springer International Publishing.

Wurz, S., S. E. Bentsen, J. Reynard, et al. 2018. "Connections, Culture and Environments Around 100 000 Years Ago at Klasies River Main Site." *Quaternary International* 495: 102–115. https://doi.org/10.1016/j.quaint.2018.03.039.

Wurz, S., R. Pickering, and S. M. Mentzer. 2022. "U-Th Dating, Taphonomy, and Taxonomy of Shell Middens at Klasies River Main Site Indicate Stable and Systematic Coastal Exploitation by MIS 5c-d." *Frontiers in Earth Science* 10: 1001370. https://doi.org/10.3389/feart.2022.1001370.

Wurz, S., N. J. le Roux, S. Gardner, and H. J. Deacon. 2003. "Discriminating Between the End Products of the Earlier Middle Stone Age Sub-Stages at Klasies River Using Biplot Methodology." *Journal of Archaeological Science* 30: 1107–1126.

Supporting Information

Additional supporting information can be found online in the Supporting Information section.

15206548, 2025, 2, Downloaded from https://onlinelibrary.wiley.com/doi/10.1002/gea.70005 by University Of Witwatersrand, Wiley Online Library on [22/10/2025]. See the Terms and Conditions (https://onlinelibrary.wiley.com/terms-and-conditions) on Wiley Online Library for rules of use; OA articles are governed by the applicable Creative Commons License